

# Bachelor's Degree Final Project

**Bachelor's Degree in Industrial Technology  
Engineering**

## **Control of a converter for photovoltaic plants**

June 15th, 2020

**Author:** Jordi Villaret Soldado

**Director:** Marc Cheah Mañé

**Deadline:** June 2020



Escola Tècnica Superior

d'Enginyeria Industrial de Barcelona



# ETSEIB



**CITCEA**



## Abstract

This project presents a model of the process involved in obtaining electrical energy from sunlight. The solar energy is a growing resource of energy, so it has been analyzed its process of conversion for a better understanding. It is intended to expose in the clearest way a photovoltaic system with its most essential elements. With the software package Matlab/Simulink, a photovoltaic array and a VSC power converter connected to the grid will be modeled. They will be studied separately and together, exposing its model blocks and equations, implementing different control variables in order to examine the variations in the system conduct, obtaining finally a way to maximize the power generated by the system.

## Contents

1. Glossary .....	5
2. Preface .....	8
2.1. Origin of the project .....	8
2.2. Motivations .....	9
2.3. Previous Requirements .....	9
3. Introduction .....	10
3.1. Objectives and scope .....	12
3.2. Project tasks .....	13
4. Model of voltage source converter .....	14
4.1. Grid converter control .....	15
4.1.1. AC side of the equivalent converter .....	16
4.1.2. Phase Locked Loop .....	18
4.1.3. Reference computation .....	23
4.1.4. Current loop control .....	25
4.2. Simulation results / DC side of the converter .....	27
4.2.1. Storage system .....	27
4.2.2. Renewable generation system .....	28
5. Model of generalized photovoltaic array .....	34
5.1. PV array operation .....	34
5.2. PV array model .....	35
5.2.1. PV array connected to a DC voltage source .....	36
5.2.2. Adaptation of the PV model .....	40
5.2.3. Adapted PV array connected to VSC-converter .....	42

---

5.3.	Maximum power point tracking (MPPT) .....	44
5.3.1.	Presentation of the MPPT algorithm .....	44
5.3.2.	VSC connected to the PV array with MPPT .....	46
6.	Environmental Impact .....	54
7.	Economic Study .....	55
8.	Conclusions .....	56
9.	Acknowledgements .....	57
10.	References .....	58

## 1. Glossary

$a$  → diode ideality constant

$C$  [F] → capacitance of the capacitor

$E_{DC}$  [V] → real DC bus voltage

$E_{DC}^*$  [V] → DC bus voltage reference

$E_g$  [eV] → bandgap energy of the semiconductor

$E_m$  [V] → admitted peak voltage value

$G$   $\left[\frac{W}{m^2}\right]$  → irradiation on the device surface

$G_n$   $\left[\frac{W}{m^2}\right]$  → nominal irradiation

$I$  [A] → net cell current

$I_0$  [A] → diode saturation current

$I_{0,n}$  [A] → nominal diode saturation current

$I_{abc}$  [A] → three – phase AC current in the abc frame

$I_{DC}$  [A] → DC current passing through the capacitor

$I_{DCI}$  [A] → DC current of the converter's DC side source

$I_{DCm}$  [A] → real DC current coming from the external current source

$I_{DCm}^*$  [A] → DC current reference of the external current source

$I_m$  [A] → PV array model current

$I_{mp}$  [A] → current in the maximum power point

$i_{qd0}$  [A] → three – phase AC current in the qd0 frame

$i_q^*$ ,  $i_d^*$  [A] → current references in qd0 frame

$I_{pv}$  [A] → light – generated current

$I_{pv,n}$  [A] → light – generated current at the nominal conditions

$k \left[ \frac{J}{K} \right] \rightarrow$  Boltzmann constant

$K_I \left[ \frac{A}{K} \right] \rightarrow$  the shortcircuit current/temperature coefficient

$K_{ic} \rightarrow$  integral constant of the current controller

$K_{iDC} \rightarrow$  integral constant of the DC voltage regulator controller

$K_p \rightarrow$  proportional constant of the PLL – PI controller

$K_{pc} \rightarrow$  proportional constant of the current controller

$K_{pDC} \rightarrow$  proportional constant of the DC voltage regulator controller

$l_l [mH] \rightarrow$  inductance value

$N_p \rightarrow$  number of cells connected in parallel

$N_s \rightarrow$  number of cells connected in series

$P [W] \rightarrow$  active power produced by the PV array

$P^* [W] \rightarrow$  active power reference

$P_{ac} [W] \rightarrow$  active power exchanged between the converter and the grid in the AC side

$P_C^* [W] \rightarrow$  active power injected to the capacitor

$P_{DC} [W] \rightarrow$  active DC bus power, measured before the capacitor

$q [C] \rightarrow$  electron charge

$Q^* [VAr] \rightarrow$  reactive power reference

$r_l [\Omega] \rightarrow$  inductance equivalent resistance

$R_s [\Omega] \rightarrow$  equivalent series resistance of the array

$R_p [\Omega] \rightarrow$  equivalent parallel resistance of the array

$T [K] \rightarrow$  actual temperature

$t [s] \rightarrow$  instant of time in the corresponding simulation

$T_n [K] \rightarrow$  nominal temperature

$[T_{qd0}] \rightarrow$  Park transformation tensor

$V [V] \rightarrow$  external cell voltage

$V_{l,0} [V] \rightarrow$  AC voltage of the converter neutral

$V_{l,abc} [V] \rightarrow$  three – phase AC voltage of the converter in the abc frame

$V_{l,qd0} [V] \rightarrow$  three – phase AC voltage of the converter in the qd0 frame

$v_{lq}^*, v_{ld}^* [V] \rightarrow$  converter AC voltage references in qd0 frame

$V_{mp} [V] \rightarrow$  voltage in the maximum power point

$V_t [V] \rightarrow$  thermal voltage of the array

$V_{z,0} [V] \rightarrow$  AC voltage of the utility grid neutral

$V_{z,abc} [V] \rightarrow$  three – phase AC voltage of the utility grid in the abc frame

$V_{z,qd0} [V] \rightarrow$  three – phase AC voltage of the utility grid in the qd0 frame

$V_{z,\alpha\beta0} [V] \rightarrow$  three – phase AC voltage of the utility grid in the  $\alpha\beta0$  frame

$\Delta V [V] \rightarrow$  variations in the  $E_{DC}^*$  of the MPPT algorithm

$\theta [rad] \rightarrow$  grid angle

$\xi \rightarrow$  dumping ratio of the system

$\xi_E \rightarrow$  desired dumping ratio of the DC voltage loop

$\tau [s] \rightarrow$  closed loop time constant of the electrical system

$\tau_{PLL} [s] \rightarrow$  PLL time constant

$\omega_E [rad/s] \rightarrow$  desired angular velocity of the DC voltage loop

$\omega_e [rad/s] \rightarrow$  angular velocity of the electrical grid

$\omega_n [rad/s] \rightarrow$  angular velocity of the system



## 2. Preface

### 2.1. Origin of the project

Throughout my life, I have been very interested in renewable energy and how it works. It is well-known that green energies are highly important to take care of the planet because of global warming effects, which are getting worse year by year, and one way to deal with them is to change the sources of energy. The bachelor final thesis is still a school project, so I felt that it was a great opportunity for me to learn more about these kinds of energy generation.

My truth interest in getting deeper into the renewable energy's world appeared at the end of 2019. I was doing a project about how could we be able to reduce the polluting emissions of the motorbikes, as it was going to be introduced a law in Barcelona which would deny the circulation in Catalonia's capital of any motorbike older than twenty years old because of the pollution they emit. The reason to initiate the project we did was to keep those people from having to get rid of their vehicles, but the final purpose of all the work was to create a way to make the environment cleaner.

We did our project in a subject of the last year of our degree, but we weren't the only ones who made a study where environmental issues were treated. Some of our classmates worked with the possibility to include some photovoltaic modules around the school. That caught my attention because there was a real possibility to get this project done. The project would be economically feasible, as the school would be saving money over the years. I began to wonder how the sunlight was able to be turned into the energy that would give electricity to the whole school, so my questions and my interests in renewable sources brought me to get into this actual project.

## 2.2. Motivations

To be able to understand the functionality of the photovoltaic system, the best way to get into it was by simulating all the process, from the reception of sunlight to the transmission of electricity. To be done, it would be necessary to use a tool such as *Matlab-Simulink*, a powerful software capable of simulating all the process.

For me, it was a big challenge to try to figure out how it all worked and, after all, be capable of recreating it in Simulink. During the last four years, the knowledge I have acquired about electricity is quite general, so coming to understand the workings of the whole system was a challenge as it was the use of that software, which I barely used in the entire career.

I could conclude that my main motivation for this project was to learn. Learn about all the electrical process and how could it be represented in the computer, so I could have the grounds to work in a project including photovoltaic arrays in the near future and contribute to improving the environment.

## 2.3. Previous Requirements

In this project, it would be required some previous knowledge and skills in:

- Power control
- Power systems
- Photovoltaic systems
- Renewable generation and storage systems
- System Dynamics and Automatic Control
- Electrotechnics
- *Matlab-Simulink* software

### 3. Introduction

Nowadays, there is a significant environmental crisis in which the future is compromised, as pollution continues to increase. In order to face this problem, one of the factors that must be confronted is where the energy is obtained from.

As technology has been progressing, renewable energy sources have become a real and necessary alternative to deal with the mentioned issue. As can be seen in Figure 1, although progress is being made in the world of renewable energies, they are still in a minority needed to be normalized. That's where microgrids come in. These are a group of electricity sources and loads composed of interconnected distributed energy resources. Those are so useful because they are self-controlled, working in grid-connected mode or changing to islanded mode when it's necessary so emergency power can be supplied. This means that in periods of time where renewable sources of power are not available, the microgrid could still provide the electricity needed. So, it should be a matter of time microgrids become standardized around the world.

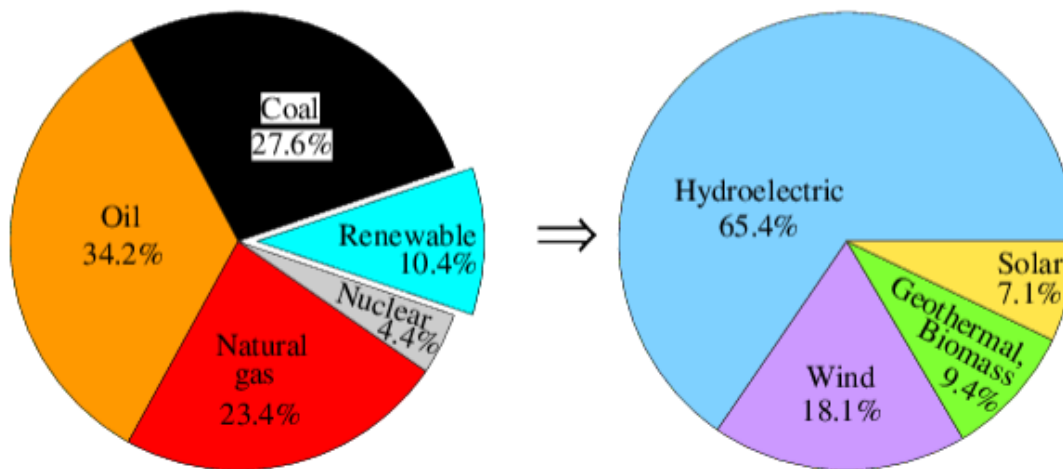


Fig. 1. Global energy consumption in 2017. [1]

Microgrids use renewable sources such as solar energy, wind energy, or biogas. As can be seen in Figure 2, the usage of renewable energy is supposed to be increasing in the next years. Although solar energy is one of the lowest in percentage usage as seen in Figure 1, it is a source that is still an emerging technology expected to continue rising as it has done over the last years, as can be seen in Figure 3.

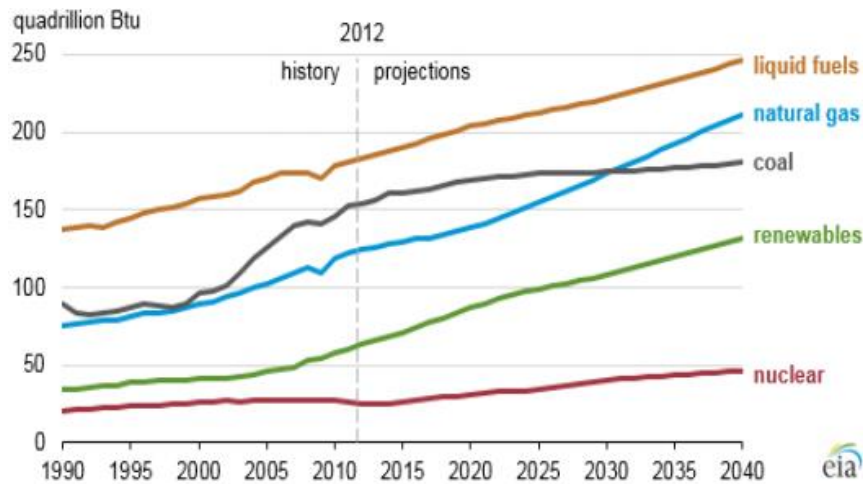


Fig. 2. World's energy historical and expected consumption. [1]

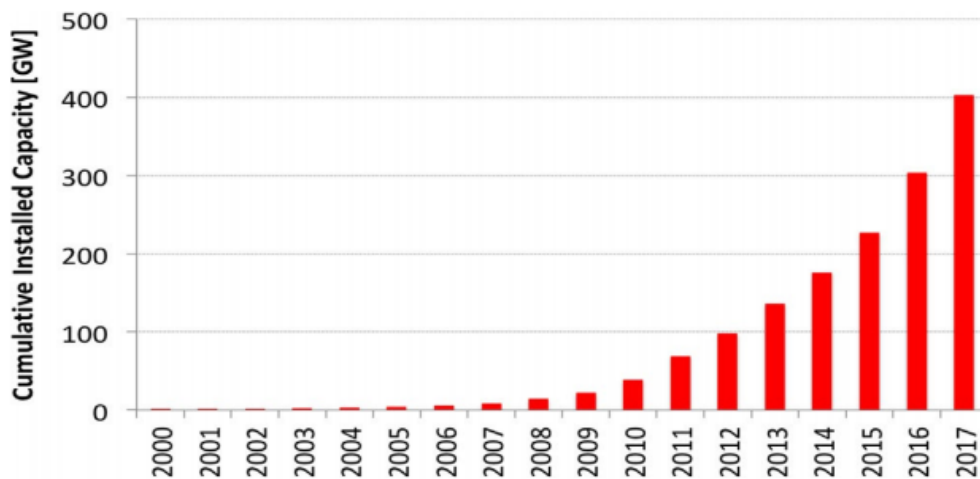


Fig. 3. Development of solar over the last years. [1]

This evolution of solar energy as a renewable source is also one of the reasons this project is focused on the process of transforming sunlight into electricity, apart from its contribution to the environment. For every thermal kWh generated, solar thermal energy only emits 2.1 grams of CO<sub>2</sub>, while the emissions of other renewable electric technologies are 14 times higher. This data was collected in a study on the carbon footprint of this technology - presented on 6 November 2019 at the IDAE -, which analyses the entire process: from the extraction of the raw materials to manufacture the panel, to its processing, transport and manufacturing process.

### 3.1. Objectives and scope

The main objective of this project is to comprehend the process of converting the energy obtained in a photovoltaic system into the grid with a standard voltage and frequency. It is wanted to analyze the whole process to implement an accurate model that would represent it. It is going to be needed a model of a power electronic converter, particularly an AC-DC converter able to work with bidirectional power, and a model of a PV array.

Basically, the objective of this work would be to represent the complex unit seen in Figure 4, composed by the microgrid and the PV array. To achieve it, first, the model of the power converter will be done, and then, the same with the shape of a PV array, so would be easier to understand the behavior of both models in different situations. Then, they will be joined to analyze the behavior of the system, and a MPPT algorithm will be implemented in order to make it more efficient.

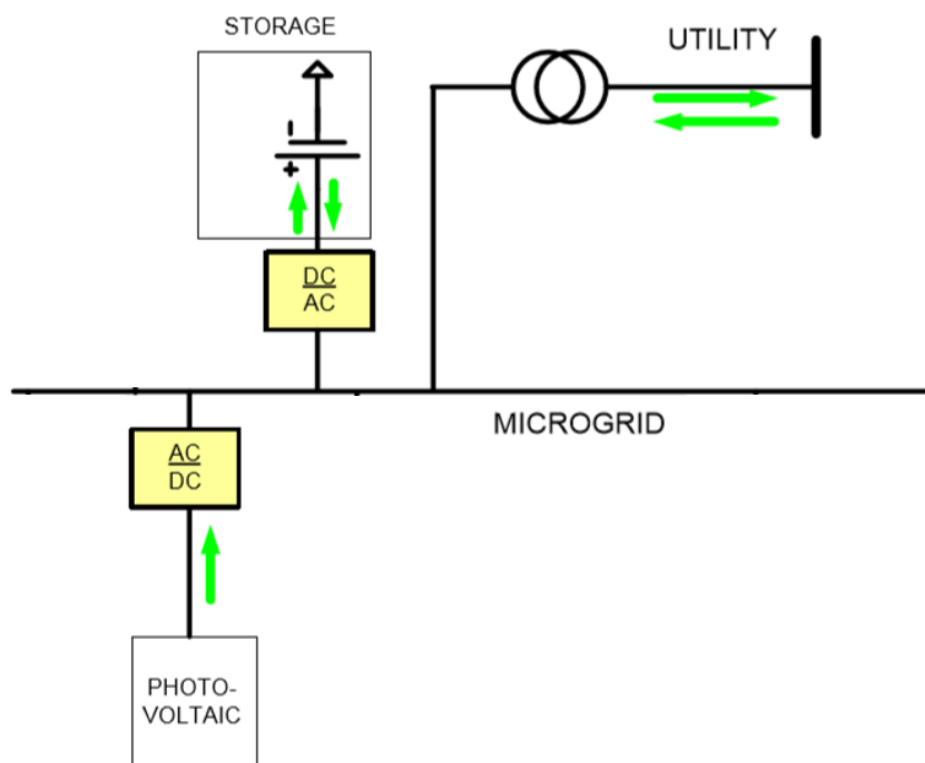


Fig. 4. Example of microgrid with the alternatives of generation or storage systems. [2]

### 3.2. Project tasks

The tasks done in this project will be focused on the behavior of the converter and the PV array. Concretely, they will be:

- Describe and design the system of the grid with the converter.
- Simulate the system working as a storage unit.
- Simulate the system emulating the usage of renewable source.
- Describe and design a simulation of photovoltaic arrays, with and without MPPT.
- Simulate changing of temperatures and irradianations in PV arrays.
- Simulate the system of the grid with the converter connected to the photovoltaic array.
- Simulate the system of the grid with the converter connected to the photovoltaic array with an MPPT, applying variations in temperature and irradiation.

This order will be followed for a correct understanding of the process.

#### 4. Model of voltage source converter

The system used in this project is based on a three-phase three-wire grid connected into a two-level Voltage Source Converter (VSC), which links the AC side with the DC side. A VSC has been chosen because it can control independently active and reactive power. That converter is an inverter composed of Insulated-Gate Bipolar Transistors (IGBT). Those are constituted by transistors, an n-type Mosfet and a pnp BJT, providing a fast switching item able to modulate any desired voltage. That high switching frequency leads to more losses, a handicap that should be taken care of.

The VSC represented in this project is composed of three branches with two IGBT each, where the middle point of every branch is connected to the grid by an inductance, shaping the AC side. The DC side of the power converter is formed by the generation or storage system, depending on the usage, connected by a shunt capacitor. The initial system is schematized in Figure 5.

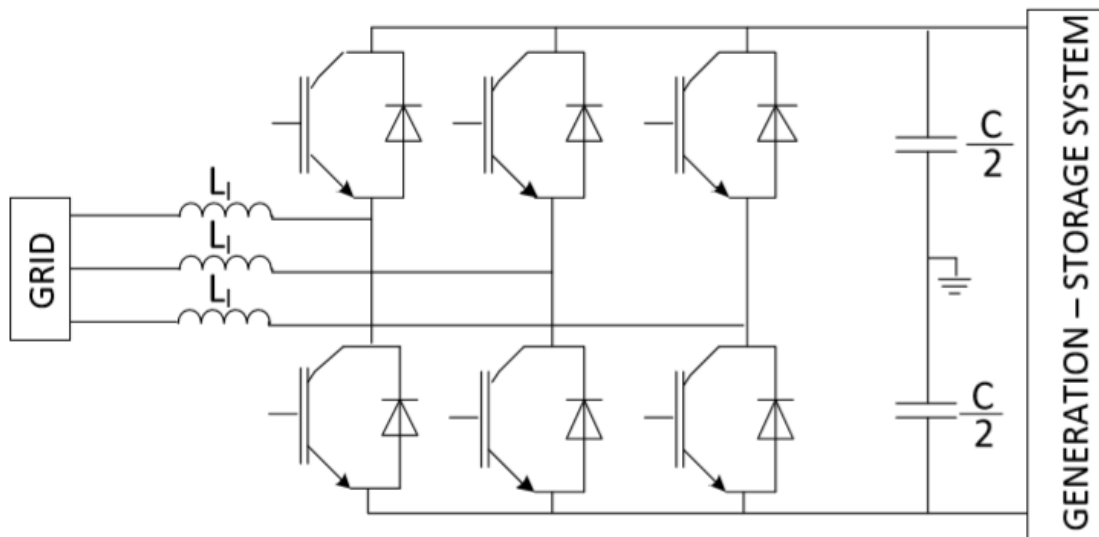


Fig. 5. Schematic of the initial system to be worked on. [2]

Active and reactive power control are going to be present in this inverter. When the converter is working with a storage system on the DC side, the active power control is needed to represent the behavior of a battery. For generation systems, active power as a variable control will be replaced by imposing a DC voltage reference to regulate the DC bus voltage and to ensure the power balance, as the power generated by the renewable source would have to be the same as the injected into the grid.

To achieve this type of control, it is more appropriate to derive the VSC converter showed in Figure 5 into a more simplified equivalent model by not implementing IGBTs. It is going to be necessary to decouple the DC and AC parts of the converter, which are going to be shown in the forthcoming chapters.

## 4.1. Grid converter control

The grid converter control scheme used in this project to obtain an adequate model to simulate is going to be shown in Figure 6, where numerous blocks responsible for keeping the system in control can be seen. All the processes are going to be explained subsequently in the sections shown in the following figure:

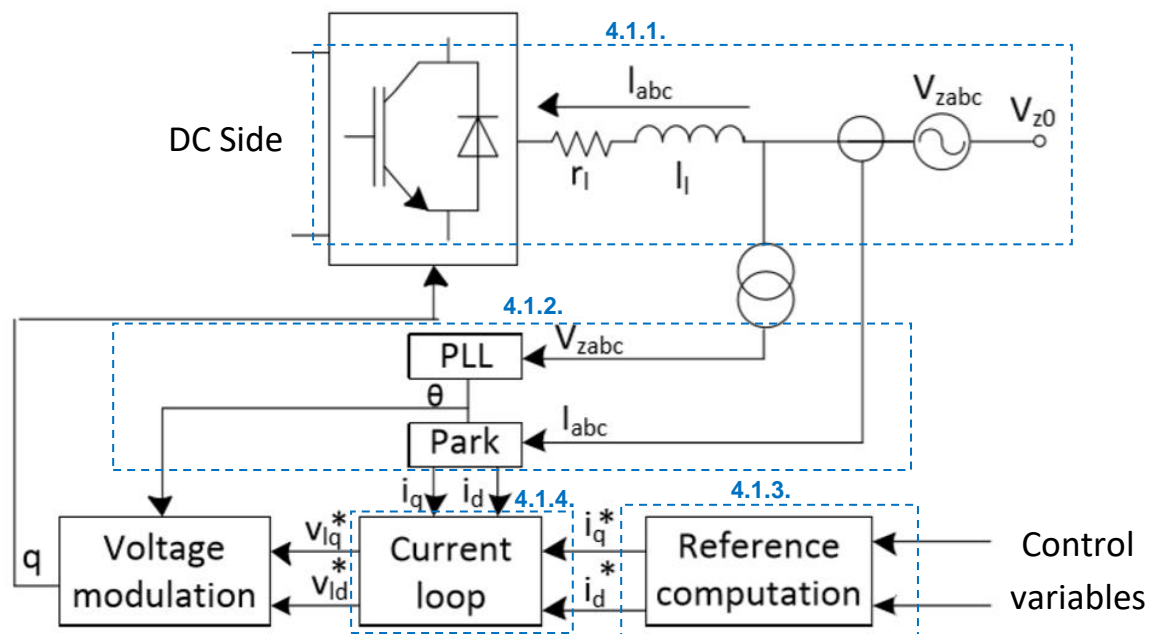


Fig. 6. Scheme of the general control of the converter's AC side. [2].

As a simplified model of the VSC is going to be used, the block "Voltage Modulation" is not going to be implemented in the following simulation. IGBTs are not used, so there will not appear the commutation between the eight different switching states, so that block is no longer necessary. A change of references would be used instead.



### 4.1.1. AC side of the equivalent converter

First, the three-phase voltage that would emulate the utility grid will be represented. It is going to be modeled with a nominal voltage as  $V_{nominal} = 230 V$  and a frequency such as  $f = 50 Hz$ . The instantaneous voltage of a balanced three-phase system in the  $abc$  reference can be expressed like [2]:

$$\begin{aligned} V_a &= \sqrt{2} \cdot V_{nominal} \cdot \cos(\omega t + \varphi) \\ V_b &= \sqrt{2} \cdot V_{nominal} \cdot \cos\left(\omega t + \varphi - \frac{2\pi}{3}\right) \\ V_c &= \sqrt{2} \cdot V_{nominal} \cdot \cos\left(\omega t + \varphi + \frac{2\pi}{3}\right) \end{aligned} \quad eq. 1.$$

Where, reminding  $\omega = 2\pi f$ ,  $\theta = \int \omega dt$  and imposing  $\varphi = 0$ , the three-phase voltage is completely defined. It can be modeled in Simulink as:

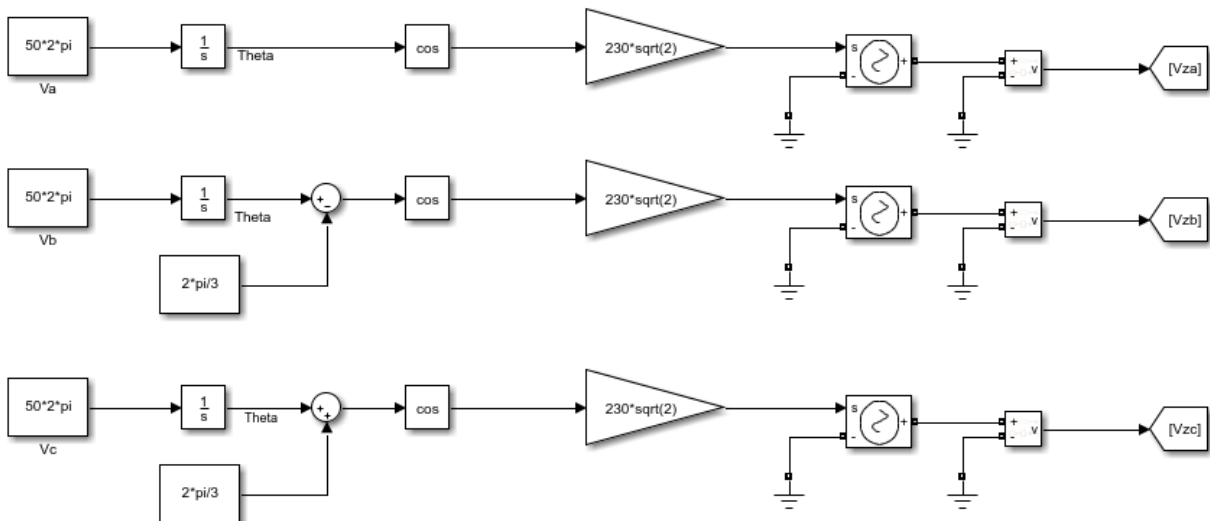


Fig. 7. Representation of the three-phase voltage of the utility grid in abc reference.

Once the utility grid voltage obtained with the model of Figure 7 is defined, it is going to be displayed the connection between the grid and the converter. Those are connected by a resistance, which would represent the inductance equivalent resistance, and an inductance. That can be a parallelism with the link mentioned previously in 4., where the IGBTs were connected to the grid by inductances, necessary to guarantee a good linkage. The current that flows through the inductances is going to be the AC current of the three-phase AC bus.

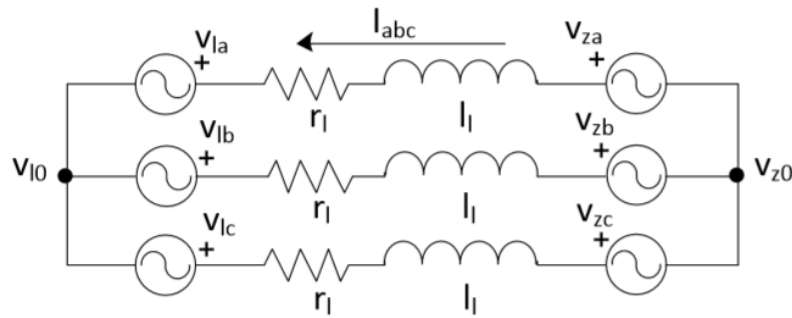


Fig. 8. Equivalent model of the AC side of the system. VSC converter and three-phase grid connected. [2]

All the simulations are going to be done using the same values of resistance and inductance. Those are  $r_l = R = 0.5 \Omega$  and  $l_l = L = 5.4 \text{ mH}$  [2]. The equivalent model showed in Figure 8 represented in the simulation would be the following one:

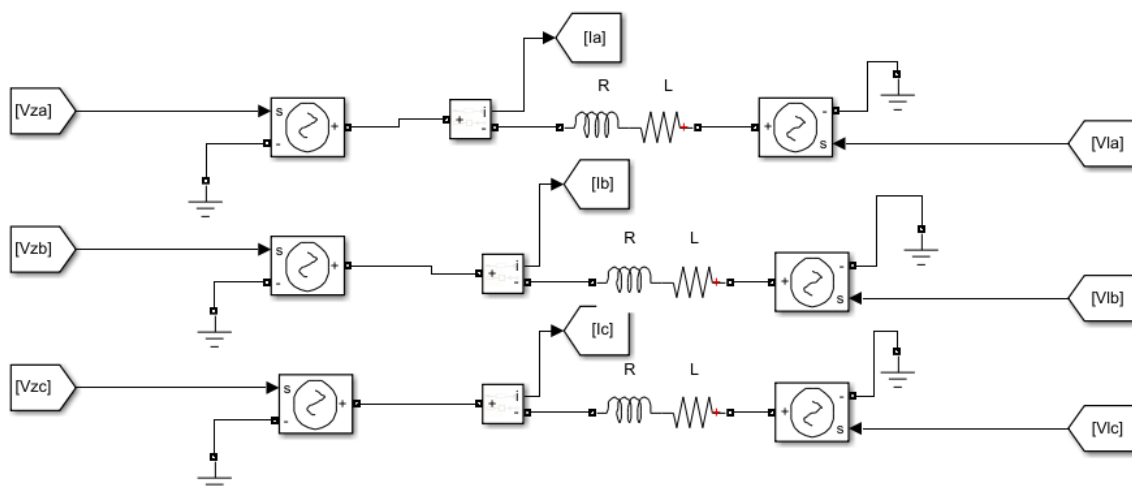


Fig. 9. Representation of the model presented in Figure 8 in Simulink.

In the system presented in Figure 9, the values defined are the three-phase grid voltage and the resistance and inductance. Neither the AC currents nor the converter voltage are still known. Their value would be defined when the loop is closed by using all the blocks presented before in the section 4.1..

### 4.1.2. Phase Locked Loop

Once  $V_{z,abc}$  and  $I_{abc}$  have been presented, the next step would be to make them profitable for the following blocks. For the controller design, it would be useful to have constant values to work with. At that point, both voltage and current are expressed in  $abc$  frame, which describes a non-constant signal. In order to achieve a constant value, the Park transformation is going to be used.

The Park transformation is based on the Clarke transformation and a rotation of a concrete  $\theta$ .

The **Clarke transformation** is a mathematical conversion with the purpose of simplifying the signals to use. It transforms a signal in the  $abc$  frame into a signal in a new orthogonal reference frame defined as  $\alpha\beta 0$ . It turns three-phase quantities onto two stationary axes. The comparison between the voltage grid described previously in  $abc$  and  $\alpha\beta 0$  frame is shown in Figure 10.

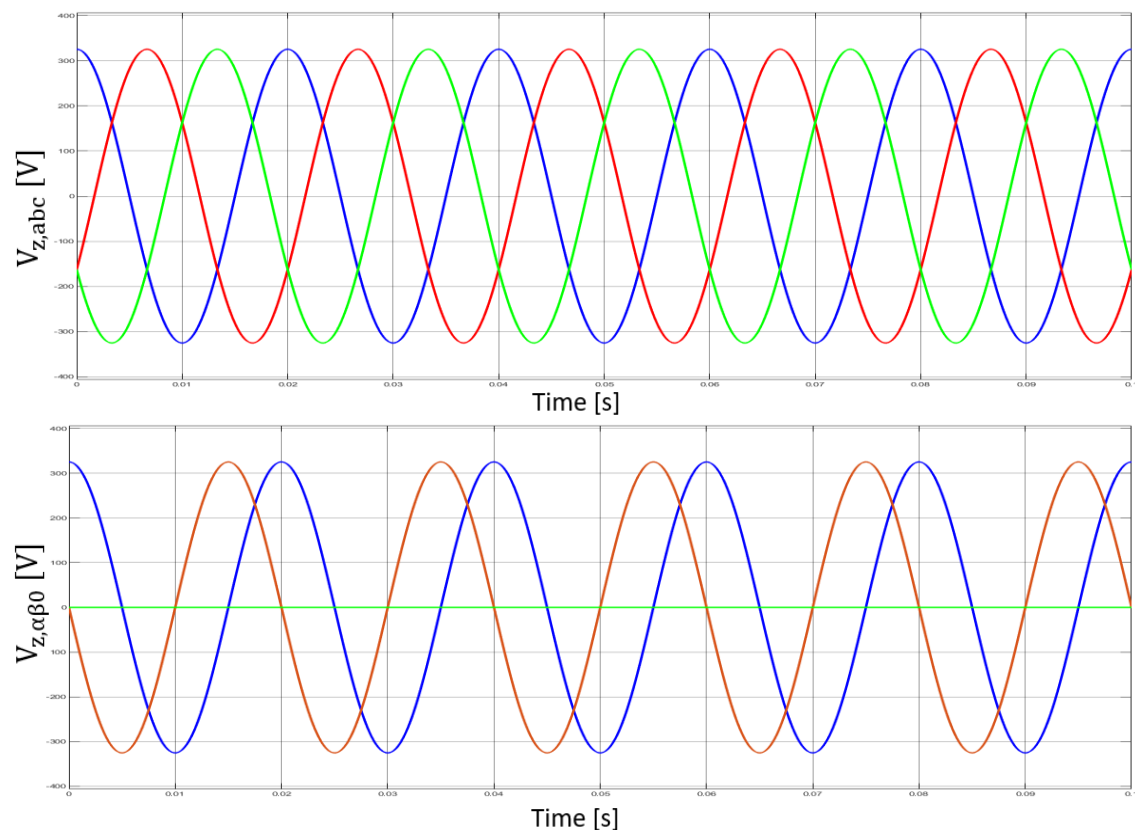


Fig. 10. Comparison of  $abc$  reference frame, which corresponds to image on top, with the  $\alpha\beta 0$  orthogonal reference frame, image of the bottom.

The new coordinates  $\alpha\beta 0$  still have an oscillatory nature, which is still not very useful for the behavior of the converter. A **rotation of a concrete angle  $\theta$**  is needed to achieve constant values.

When the Clarke transformation, which changes three-phase onto two axes, and the rotation are applied together, it is obtained the synchronous reference frame. That process is also called as **Park transformation**, which will obtain transformed quantities in the  $qd0$  frame. In Figure 11 can be seen the implemented change of references, from  $abc$  to  $\alpha\beta 0$  to  $qd0$ .

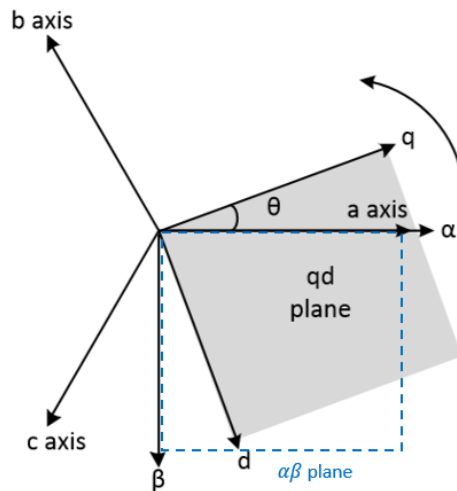


Fig. 11. Transition from the  $abc$  reference to  $qd0$  by using the Park transformation. [2]

To implement the Park transformation, it is used a tensor to change from the reference frame of the three-element vector to the direct-quadrature-zero ( $qd0$ ) frame. The tensor is going to be presented as:

$$[x_{qd0}] = [T_{qd0}][x_{abc}] \quad \text{eq. 2.}$$

It depends on the  $\theta$  rotation, and when it is developed it can be expressed as:

$$[T_{qd0}(\theta)] = \frac{2}{3} \begin{bmatrix} \cos(\theta) & \cos(\theta - \frac{2\pi}{3}) & \cos(\theta + \frac{2\pi}{3}) \\ \sin(\theta) & \sin(\theta - \frac{2\pi}{3}) & \sin(\theta + \frac{2\pi}{3}) \\ \frac{1}{2} & \frac{1}{2} & \frac{1}{2} \end{bmatrix} \quad \text{eq. 3.}$$

This tensor is only useful when it is needed to pass from  $abc$  frame to  $qd0$ , as can be seen in Figure 12. In the Simulink simulation, the  $0$ -coordinate has been skipped due to no real use of that signal.

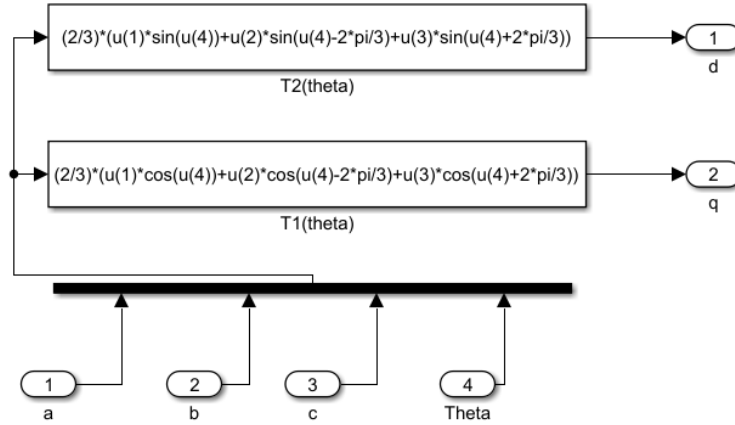


Fig. 12. Model of the tensor  $[T_{qd0}]$  to obtain  $qd$  signals.

When what is needed is not to transform  $abc$  into  $qd0$  but  $qd0$  into  $abc$ , the inverse of the tensor shown in eq. 3. would be necessary. It can be expressed as:

$$[x_{abc}] = [T_{qd0}]^{-1} [x_{qd0}] \quad \text{eq. 4.}$$

Where

$$[T_{qd0}(\theta)]^{-1} = \begin{bmatrix} \cos(\theta) & \sin(\theta) & 1 \\ \cos(\theta - \frac{2\pi}{3}) & \sin(\theta - \frac{2\pi}{3}) & 1 \\ \cos(\theta + \frac{2\pi}{3}) & \sin(\theta + \frac{2\pi}{3}) & 1 \end{bmatrix} \quad \text{eq. 5.}$$

Which is going to be modeled in Simulink in a similar way as the non-inverse tensor, shown in Figure 13:

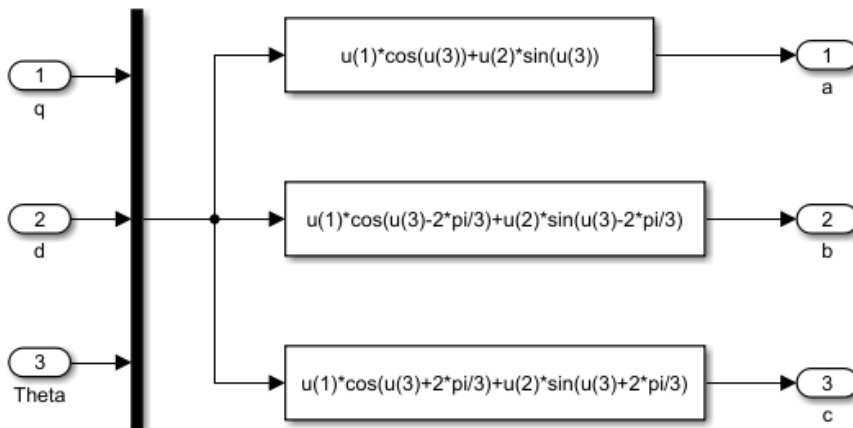


Fig. 13. Model of the tensor  $[T_{qd0}(\theta)]^{-1}$  to obtain  $abc$  signals.

As it can be seen in those models, the specific value of the angle Theta ( $\theta$ ) is needed. That's where the **Phase Locked Loop (PLL)** takes part. This block is used to determine the necessary theta angle  $\theta$ , the grid angle, required to execute the change of references. It is also useful to obtain the angular velocity  $\omega_e$ , which is going to be needful in the current loop, explained later on.

A PLL is an electronic circuit based on the Park transformation and a PI controller. It consists in a feedback of the  $V_{z,d}$  signal with a 0-reference filtered by the controller to stabilize this voltage to 0. The output of the block is the theta value, which is used to close the loop to complete the Park transformation in an iterative way. The PLL model used in the simulation is presented in Figure 14:

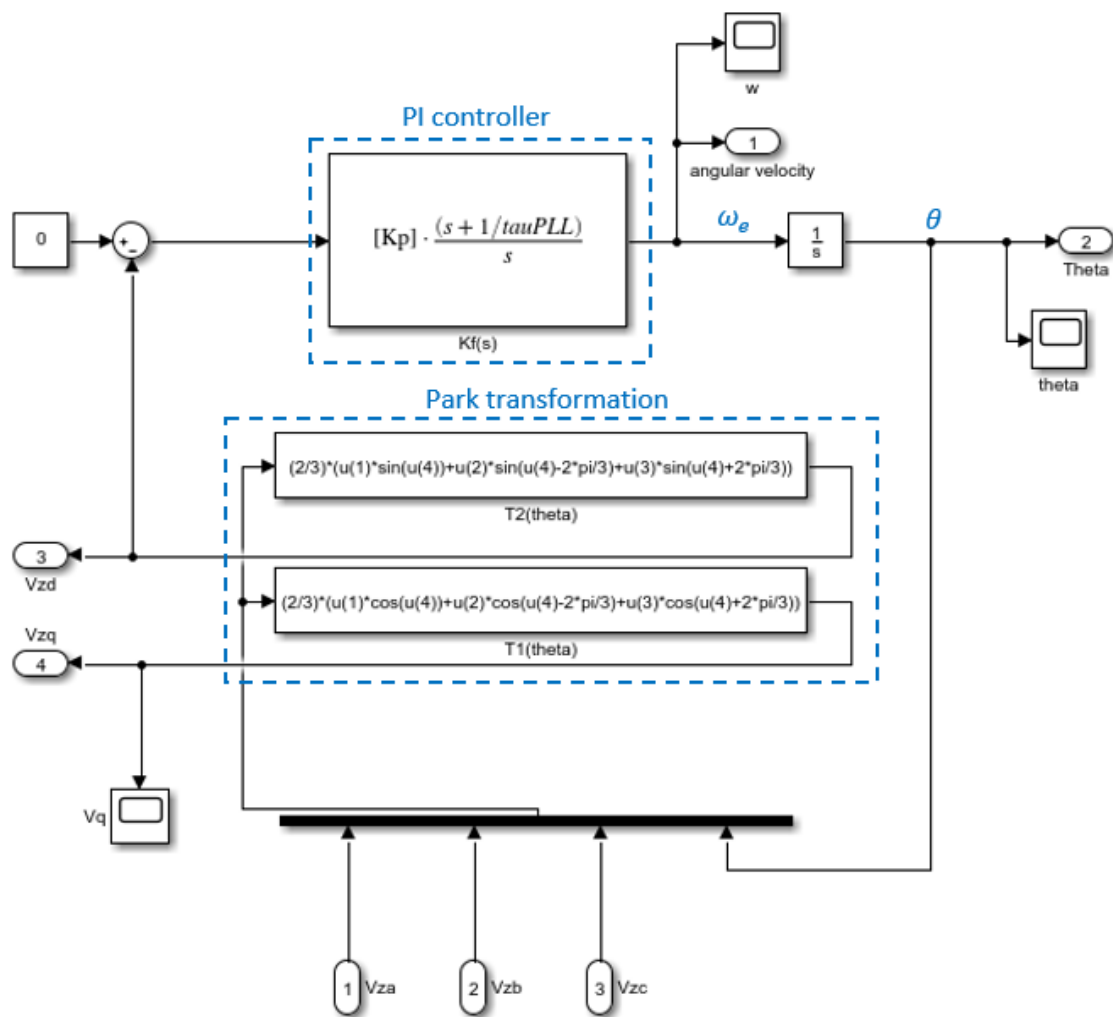


Fig. 14. Model simulated of the Phase Locked Loop.

The PI controller is mainly implemented to achieve the expected value of  $V_{z,d}$ . The values  $K_p$  and  $\tau_{PLL} = \tau_{PLL}$  shown in the previous figure are obtained by using the following equations [2]:

$$\omega_n = \sqrt{\frac{K_p E_m}{\tau_{PLL}}} \quad \xi = \frac{\sqrt{\tau_{PLL} K_p E_m}}{2} \quad \text{eq. 6, 7.}$$

Those equations are formulated after analyzing the second-order system behavior obtained in this loop. The damping ratio is a parameter that describes how rapidly the oscillations decay from one bounce to the next, while the natural frequency is the frequency of oscillation of the system without damping. These are design parameters, which could be modified due to better dynamics of the loop.

In this case,  $E_m = 230 \cdot \sqrt{2} \text{ V}$ ,  $\xi = 0.707$  and  $\omega_n = 418 \text{ rad/s}$  are imposed. These are given in [2], used to obtain the values of  $K_p$  and  $\tau_{PLL}$ .  $\tau_{PLL}$  would be the time constant of the PLL controller, which would be the time when the response achieves the 63% of the final value. It gives an idea of how fast the controller would work. According to the equations 6 and 7, the next values are determined:

$$K_p = 1,8209 \qquad \tau_{PLL} = 3,3757 \cdot 10^{-3} \text{ s}$$

At this point, PLL is completely defined.  $V_{z,qd}$ , the grid angle  $\theta$  and the angular velocity of the electrical grid  $\omega_e$  are available to be used in the further blocks.

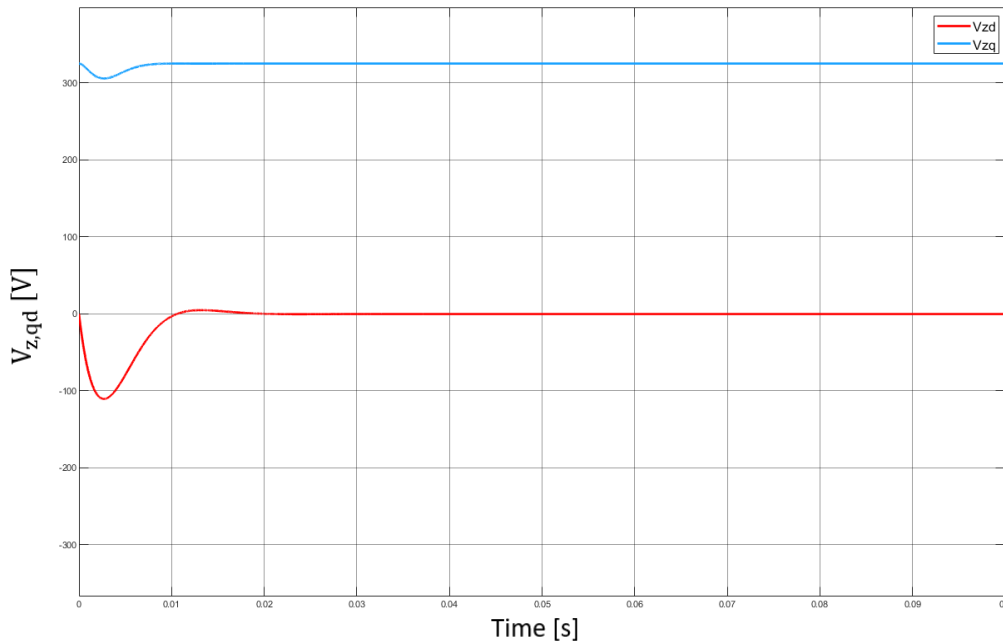


**Fig. 15. Signals obtained of  $V_{z,q}$ , the blue trace, and of  $V_{z,d}$ , the red trace.**

It can be appreciated in Figure 15 how  $V_{z,d}$  is stabilized at 0 and  $V_{z,q}$  does the same in the peak value  $E_m$ .

### 4.1.3. Reference computation

In this project, two different scenarios are going to be considered:

- Converter connected to a DC voltage source emulating a storage system.
- Converter connected to a DC current source emulating a renewable generation system.

The DC side will be explained further on, but in these two different cases different references will be contemplated.

When the **storage generation system** is represented, active and reactive power references are going to be used.

It is assumed a battery system of constant DC voltage, and the active power reference is applied in this case to emulate its behavior.

As a VSC converter is simulated, active and reactive power can be supplied and controlled independently. The reactive power will be used to acquire the current reference in the same way as the active power.

To obtain the current references from the power references, the following equations will be used [2]:

$$P^* = \frac{3}{2}(V_{z,q}i_q^* + V_{z,d}i_d^*) \quad \text{eq. 8.}$$

$$Q^* = \frac{3}{2}(V_{z,q}i_d^* - V_{z,d}i_q^*) \quad \text{eq. 9.}$$

In Figure 15, it is noticeable that  $V_{z,d}$  has the constant value of 0 when it is stabilized. Consequently, the second term of these equations will be neglected. So, the current references would be acquired in the following manner:

$$i_q^* = \frac{2 P^*}{3 V_{z,q}} \quad i_d^* = \frac{2 Q^*}{3 V_{z,q}} \quad \text{eq. 10, 11.}$$

On the other hand, when **renewable generation** is considered, reactive power as a control variable will still be assumed, but the bus voltage reference  $E_{DC}^*$  will be used instead of the active power reference.



Therefore, equations 9 and 11 will still be implemented. To acquire the reference current  $i_q^*$  through the DC voltage reference, a DC voltage regulator [2] is required. The purpose of this regulator is to stabilize the DC bus voltage, which would be the voltage the converter would externally see, to the given constant DC voltage reference, and thus ensure the power balance between the power injected to the grid and the source of the renewable generation.

That voltage control is based on the equations which relate the power and the voltage of the capacitors. The power would be proportional to the square of the voltage:

$$P_{capacitor} = \frac{1}{2} \cdot C \cdot U^2 \quad \text{eq. 12.}$$

Where  $U$  would be the voltage between the capacitor plates. This relation is why the following voltage regulator is based on the square of the DC voltages:

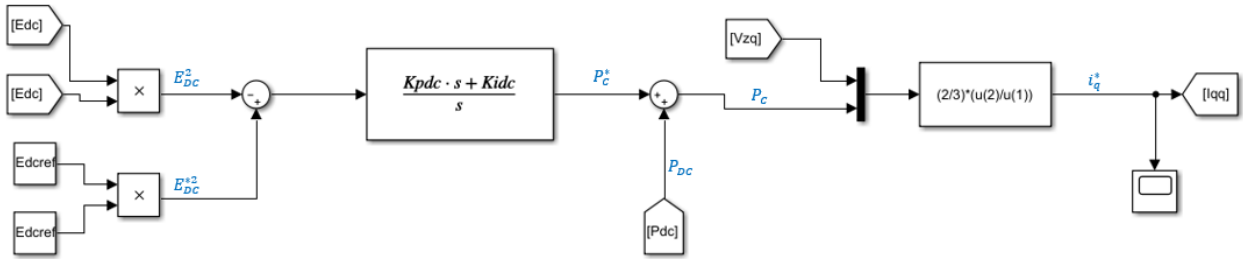


Fig. 16. Model of the DC voltage regulator.

As can be seen in Figure 16, the controller basically consists of a PI controller and the equation 10 to obtain the current reference  $i_q^*$ . There is also a perturbation,  $P_{DC}$ , which will be defined further on.

The values of the controller can be calculated with the following equations [2]:

$$K_{pDC} = C \xi_E \omega_E \quad K_{iDC} = \frac{C \omega_E^2}{2} \quad \text{eq. 13, 14.}$$

Considering  $\tau_E = 1 \cdot 10^{-3}$  s,  $\omega_E = 418,88$  rad/s and  $C = 1020 \cdot 10^{-6}$  F [2], the following values of controller constants are obtained:

$$K_{pDC} = 0,3021 \quad K_{iDC} = 89,4848$$

#### 4.1.4. Current loop control

After getting the values of the current references, current control would be used. The real current values  $i_q$  and  $i_d$  must be obtained by applying the Park transformation to the  $I_{abc}$  signal acquired in the previous Figure 9 using the tensor of Figure 12.

First, the voltage equations of the system are going to be presented [2]:

$$\begin{bmatrix} V_{z,q} \\ V_{z,d} \end{bmatrix} - \begin{bmatrix} V_{L,q} \\ V_{L,d} \end{bmatrix} = \begin{bmatrix} r_l & l_l \omega_e \\ l_l \omega_e & r_l \end{bmatrix} \begin{bmatrix} i_q \\ i_d \end{bmatrix} + \begin{bmatrix} l_l & 0 \\ 0 & l_l \end{bmatrix} \frac{d}{dt} \begin{bmatrix} i_q \\ i_d \end{bmatrix} \quad \text{eq. 15.}$$

As can be seen, the  $q$  and  $d$  components of voltages and currents are coupled. Current loop control is going to be implemented, so  $q$  and  $d$  components would be decoupled and independently controlled to obtain the suitable  $V_{L,q}$  and  $V_{L,d}$  values that would make  $i_q$  and  $i_d$  reach the respective values of the current references.

By using the voltage equations seen in eq. 15, introducing the mentioned value of  $V_{z,d}=0$  and neglecting this variable, the following current controller showed in Figure 17 will be executed:

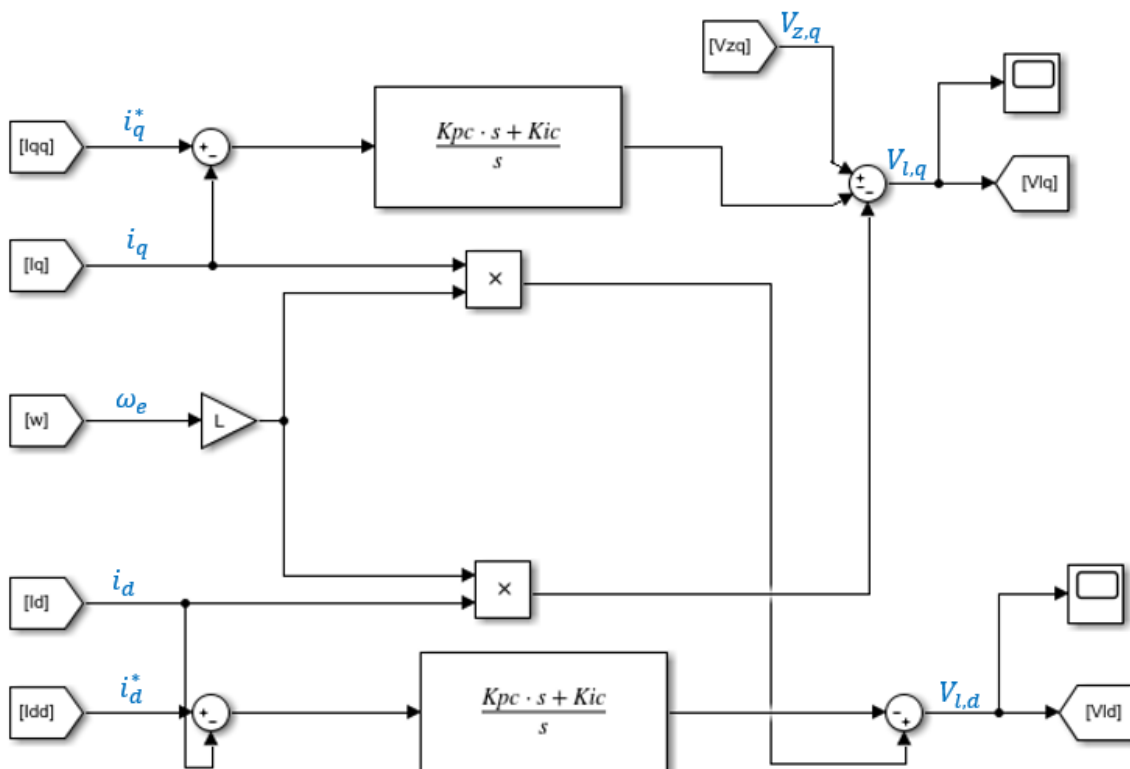


Fig. 17. Model of the current controller used in the simulation.

As in the DC voltage controller, a PI controller will be used to control both  $i_q$  and  $i_d$  so their value will be adjusted to their corresponding references with a first-order dynamics. The controller constants will be determined using [2]:

$$K_{pc} = \frac{l_l}{\tau} \qquad K_{ic} = \frac{r_l}{\tau} \qquad \text{eq. 16, 17.}$$

The value of the closed loop time constant would be chosen depending on the converter characteristics, as it is usual to define a  $\tau$  approximately 10 times faster than the converter switching frequency. In the case of the storage system simulation,  $\tau$  would be 10 ms, while when the generation renewable system is implemented,  $\tau = 1$  ms is going to be used, so a faster response should be achieved in the last case as the 63% of the final value would be expected to be raised before.

In the case of storage system simulation with  $\tau = 10$  ms:

$$K_{pc} = 0,54 \qquad K_{ic} = 50$$

In the case of renewable generation system with  $\tau = 1$  ms:

$$K_{pc} = 5,4 \qquad K_{ic} = 500$$

Once the current loop is completed, the outputs of this block will be processed. The inverse of the Park transformation will be applied in order to convert the  $qd0$  converter voltage into the  $abc$  frame by using the tensor of Figure 13. Once  $V_{l,abc}$  is obtained, the AC side of the system would be completely defined.

## 4.2. Simulation results / DC side of the converter

As has been said before, two different situations will be studied.

### 4.2.1. Storage system

When a storage system is considered, a battery system of constant DC voltage is assumed. By considering the active power as a control variable, the battery is going to be skipped in the model as the active power injected to the grid will represent the compartment of the battery. It is worth remembering this power converter can supply active power independently from reactive power.

A one-second simulation is going to be run in all simulations. The values of the control variables  $P^*$  and  $Q^*$  will be represented in the following Table 1:

Time instant [s]	Active power $P^*$ [kW]	Reactive power $Q^*$ [kVAr]
0	-2	-4
0.3	-1	0
0.5	-2	-1
0.8	-5	2
0.9	-9	-9

Table 1. Values of the references  $P^*$  and  $Q^*$ .

Some remarkable aspects of this simulation could be the comportment of the power converter voltage, which is increased in the three periods in accordance with the time reactive power is negative. That means that the reactive power flows from the outside of the power converter to the inner of the VSC.

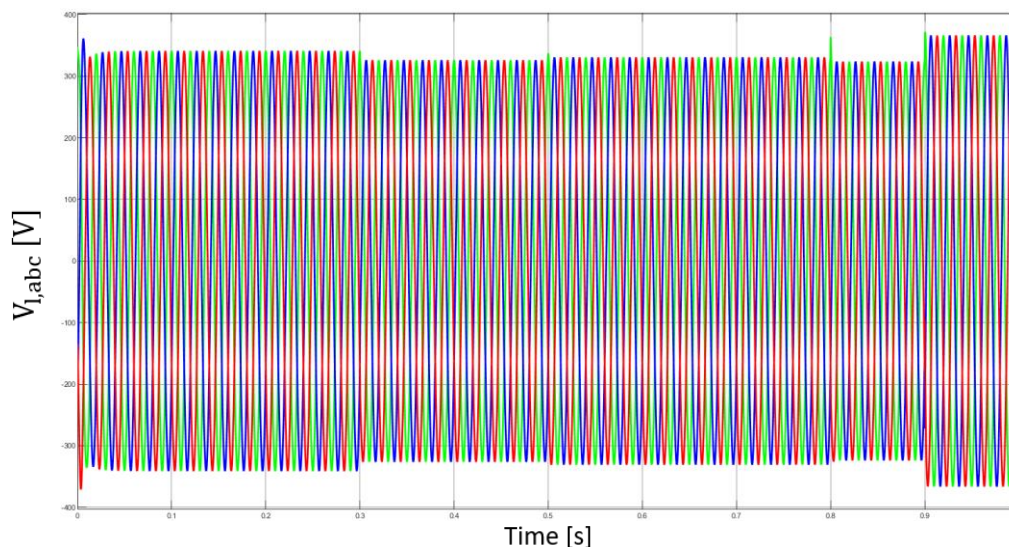


Fig. 18. Plot of  $V_{l,abc}$  signal of the storage system simulation.

As can be seen in Figure 18, when  $0 < t < 0,3s$ ,  $0,5s < t < 0,8s$  and  $0,9s < t < 1s$ , the  $V_{l,abc}$  signal is increased because of reactive power demand.

Another important aspect to take into account would be the relation between the measured currents and the power references. The bigger the power reference in absolute value would be, more current would circulate through the system, as can be appreciated in Figure 19:

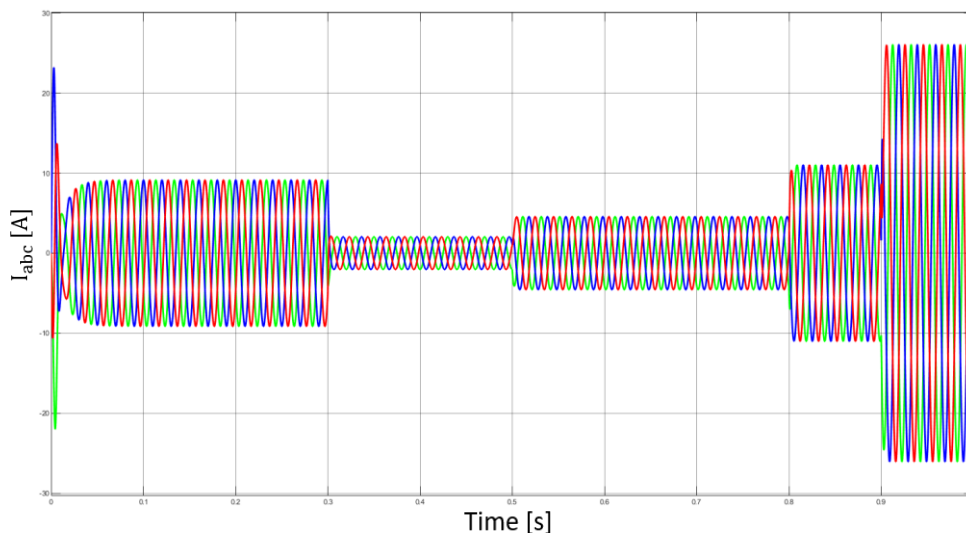


Fig. 19. Plot of  $I_{abc}$  signal of the storage system simulation.

Between  $t=0,3s$  and  $t=0,5s$  the  $abc$  current has its minimum and between  $t=0,9s$  and  $t=1s$  has its maximum. Due to the relations imposed between powers and currents in equations 8 and 9, the results obtained are coherent. In the period the current is at its lowest is when  $Q^* = 0$  and  $P^* = -1$  kW, the lowest values of power. The opposite happens with the highest of the current, which corresponds with the period when  $Q^* = -9$  kVAr and  $P^* = -9$  kW. Therefore, the results obtained in the simulation would be considered as valid.

#### 4.2.2. Renewable generation system

In order to simulate a renewable source that would be connected to the VSC, an external current source would be used.

First, the DC side of the converter must be defined, as the external source would be joined to the converter's end, as showed in Figure 20. As a simplified model is being used, the DC side of the converter would be represented as a current source and a capacitor. Both sides of the power converter would be related by guaranteeing that the active power exchanged between the VSC converter and the AC side of the grid would be the same as the active power exchanged between the AC and the DC side. By imposing this condition, power balance would be ensured.

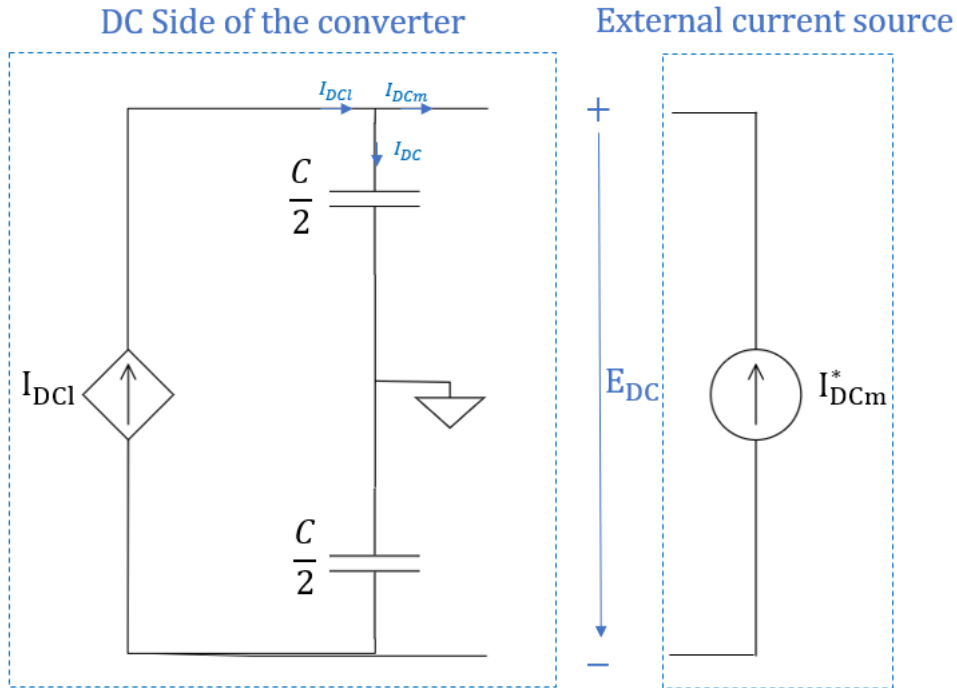


Fig. 20. Scheme of the DC side of the VSC connected to the external current source.

The mentioned relation between powers would be implemented to impose the  $I_{DCl}$  value. The power exchanged among converter and grid is going to be calculated with the following equation, considering  $V_{z,d}=0$ .

$$P_{ac} = \frac{3}{2} V_{z,q} i_q \quad \text{eq. 18.}$$

Therefore, the current of the DC source will be determined by:

$$I_{DCl} = \frac{P_{ac}}{E_{DC}} \quad \text{eq. 19.}$$

The value of the external current source will be imposed by steps, as was done in the storage system with the power references. As it has been said in the section 4.1.3., in this case, reactive power and the external DC voltage reference are the control variables. However, the current of the external source will be imposed, emulating renewable generation, which will produce changes in the generated power. The following values of Table 2 are going to be used:

Time instant [s]	DC current $I_{DCm}^*$ [A]	Reactive power $Q^*$ [kVAr]
0	5	-2
0.3	6	0
0.5	3	-3
0.8	10	0
0.9	5	-6

Table 2. Values of the references  $I_{DCm}^*$  and  $Q^*$ .

With both current sources defined, the DC voltage regulator mentioned in 4.1.3. should be implemented to regulate the  $E_{DC}$  voltage to the  $E_{DC}^*$  voltage reference, which is going to be fixed in **800 V**. The perturbation of that block,  $P_{DC}$ , will be calculated:

$$P_{DC} = E_{DC} I_{DCm} \quad \text{eq. 20.}$$

That would correspond to the DC bus power, calculated before the capacitor. To implement this block, initially the DC voltage reference would have to be used until the real DC voltage is stabilized, approximately at  $t=0,03$  s. The control of the DC voltage would guarantee the stabilization of  $E_{DC}$  to the 800 V without the perturbation causing any significant effect. The implementation of these previous expressions would be represented in the following model of Figure 21:

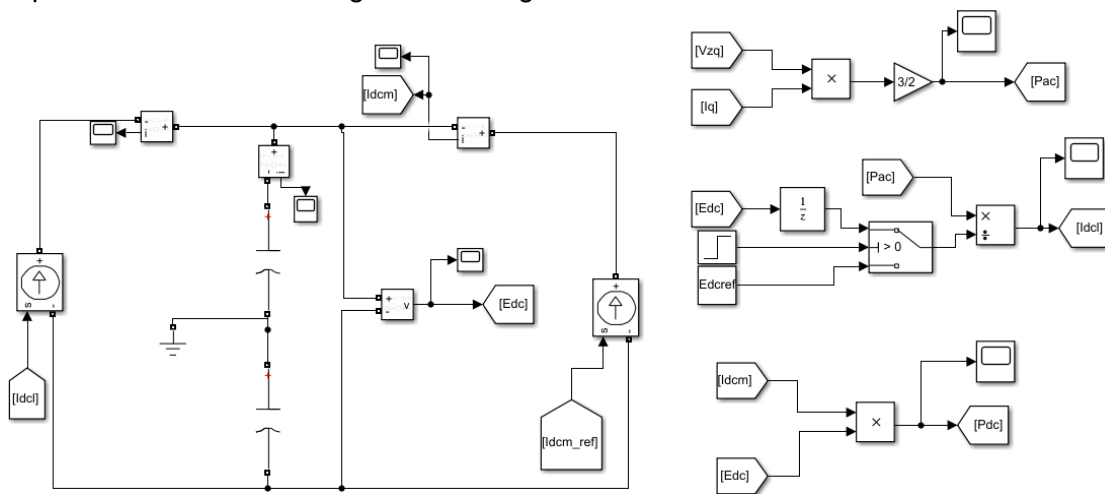


Fig. 21. Model of the DC system of a renewable generation simulation.

With the whole model explained through the project and the mentioned generation system, some remarkable results have been obtained.

It is appreciable in Figure 22 how in every  $t$  the DC current changes, the  $E_{DC}$  voltage makes a small leap until it gets stabilized again to the reference value thanks to the implemented voltage regulator.

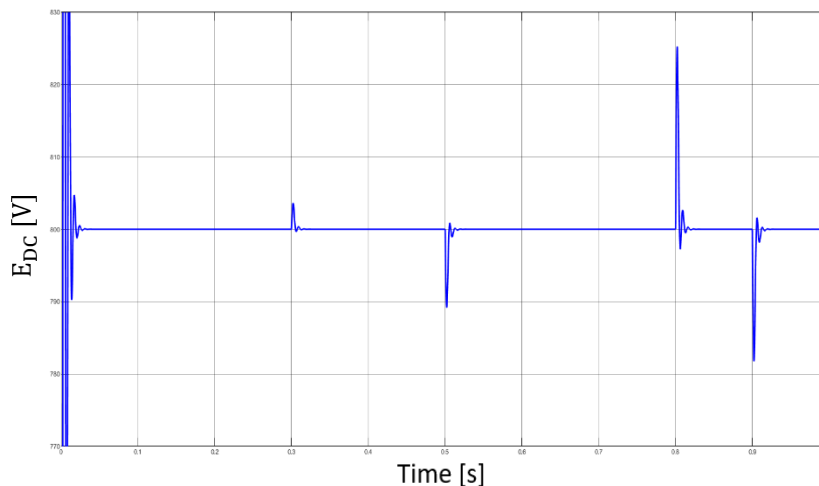


Fig. 22. Plot of the  $E_{DC}$  signal in the renewable generation simulation.

It can be appreciated that the greater the change of current is, the higher the peak of DC voltage would be. The greatest change of current occurs in  $t=0.8$  ms, where a current gradient of 7 A is injected. It can be seen that it corresponds to the highest peak of the previous plot. In  $t=0.1$  ms, the current increases just 1 A, so the contrast between both peaks can be observed.

By analyzing the DC currents of the model, it is possible to appreciate in Figure 23 how the capacitor blocks the flow of DC current as soon as the system is stabilized due to its insulating layer. The voltage across its plates is allowed to be measured instead, which corresponds to the DC bus voltage.

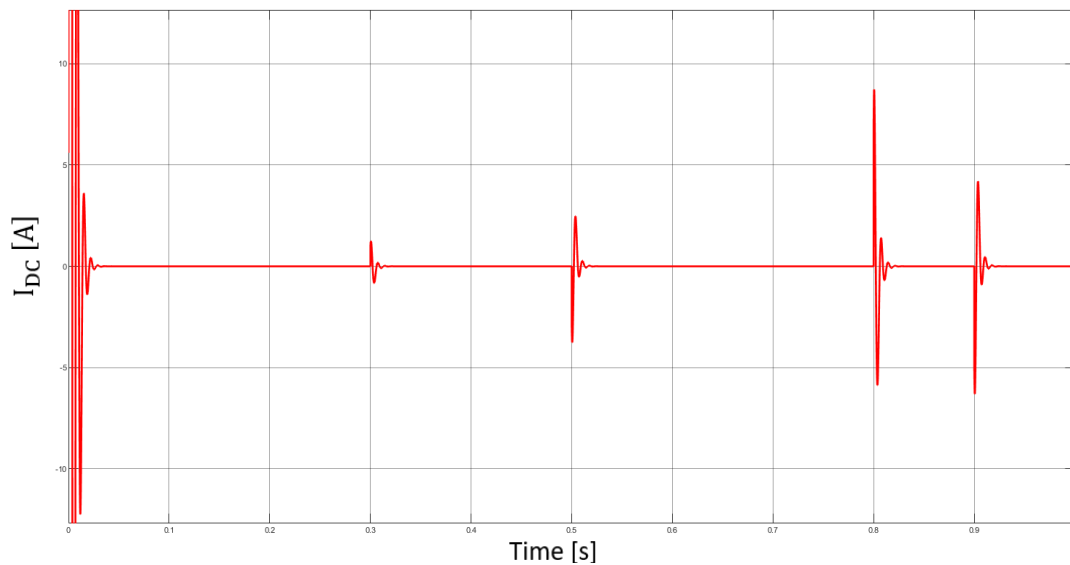


Fig. 23. Plot of the  $I_{DC}$  signal in the renewable generation simulation.

A similar comportment as the  $E_{DC}$  voltage is observed, but instead of getting stabilized to a reference value (800 V), the current through the capacitors will tend to be zero as it gets blocked when the transitory period is over.

Consequently,  $I_{DCI}$  will be the same as the stair reference signal given to define the external current source  $I_{DCm}^*$ , as can be seen in Figure 24.

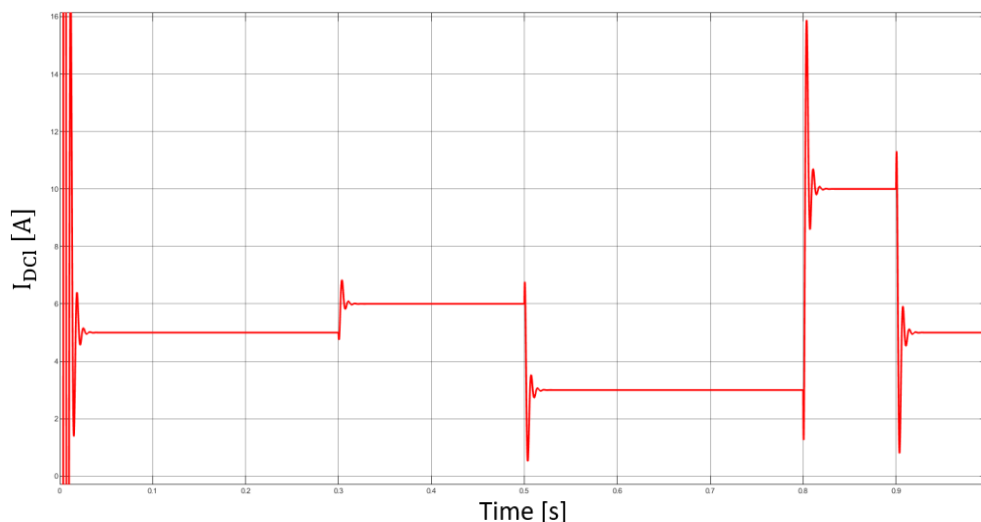


Fig. 24. Plot of  $I_{DCI}$  in the renewable generation simulation.



The behavior of the AC currents in the synchronous frame are also interesting to be analyzed. According to equations 10 and 11,  $i_q$  current is determined by the DC current, as it is directly related to the active power, and  $i_d$  is related to the reactive power, both references in this system.

The quadrature reference of the AC current,  $i_q^*$ , is obtained through the DC voltage regulator. As it has a second-order dynamics,  $i_q^*$  would have the comportment of a second-order system and the same would happen with  $i_q$ , as it would try to follow the reference thanks to the current loop. Their second-order dynamics can be seen in the Figure 25.

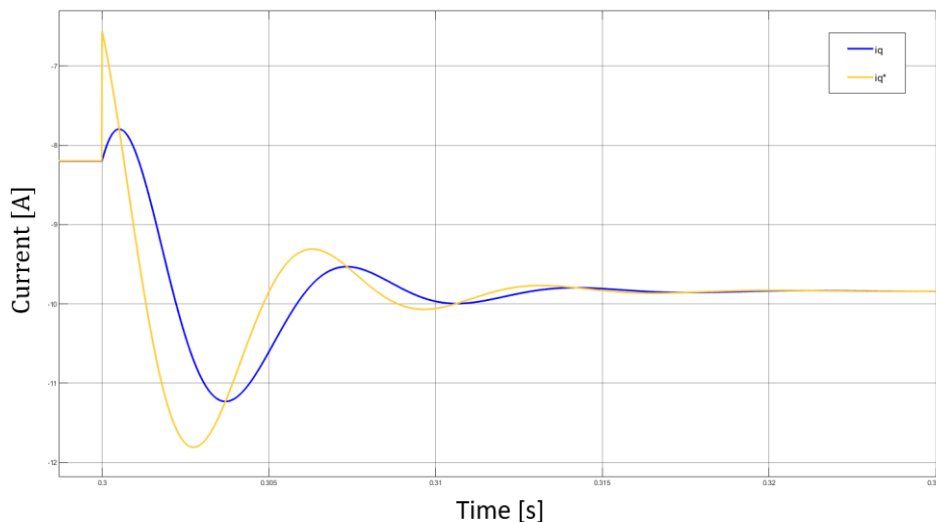


Fig. 25. Signals obtained of  $i_q$ , the blue trace, and of  $i_q^*$ , the orange trace.

With the direct signal, it is simpler. As the reference is directly obtained with the reactive power reference applying equation 11, the second-order dynamics of the voltage regulator won't be present. Instead, the real  $i_d$  value would have a first-order dynamics behavior, acquired from the PI controller of the current loop control, which urged a first-order dynamics to the signal. That conduct can be seen in the following plot of Figure 26, where both reference and real currents are showed:

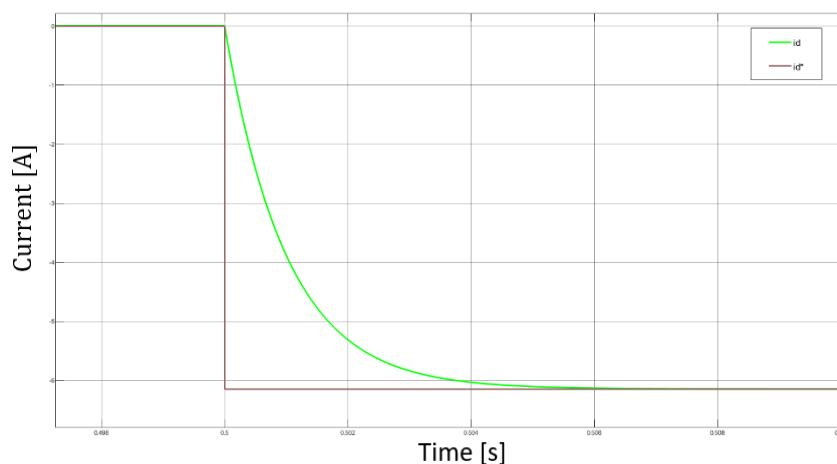


Fig. 26. Signals obtained of  $i_d$ , the green trace, and of  $i_d^*$ , the brown trace.

It is remarkable to say that this first-order behavior seen above, it is the same conduct both  $i_q$  and  $i_d$  take in the simulation done before when a storage system was considered, as there is no DC voltage regulator.

To conclude with this system, an analysis of active powers is going to be studied. As have been seen in Figure 23, the current going through the capacitors is null, so there won't be active power considered in the capacitors, as it is obvious. So, as there won't be losses of power through the process, the following powers showed in Figure 27 will be obtained:

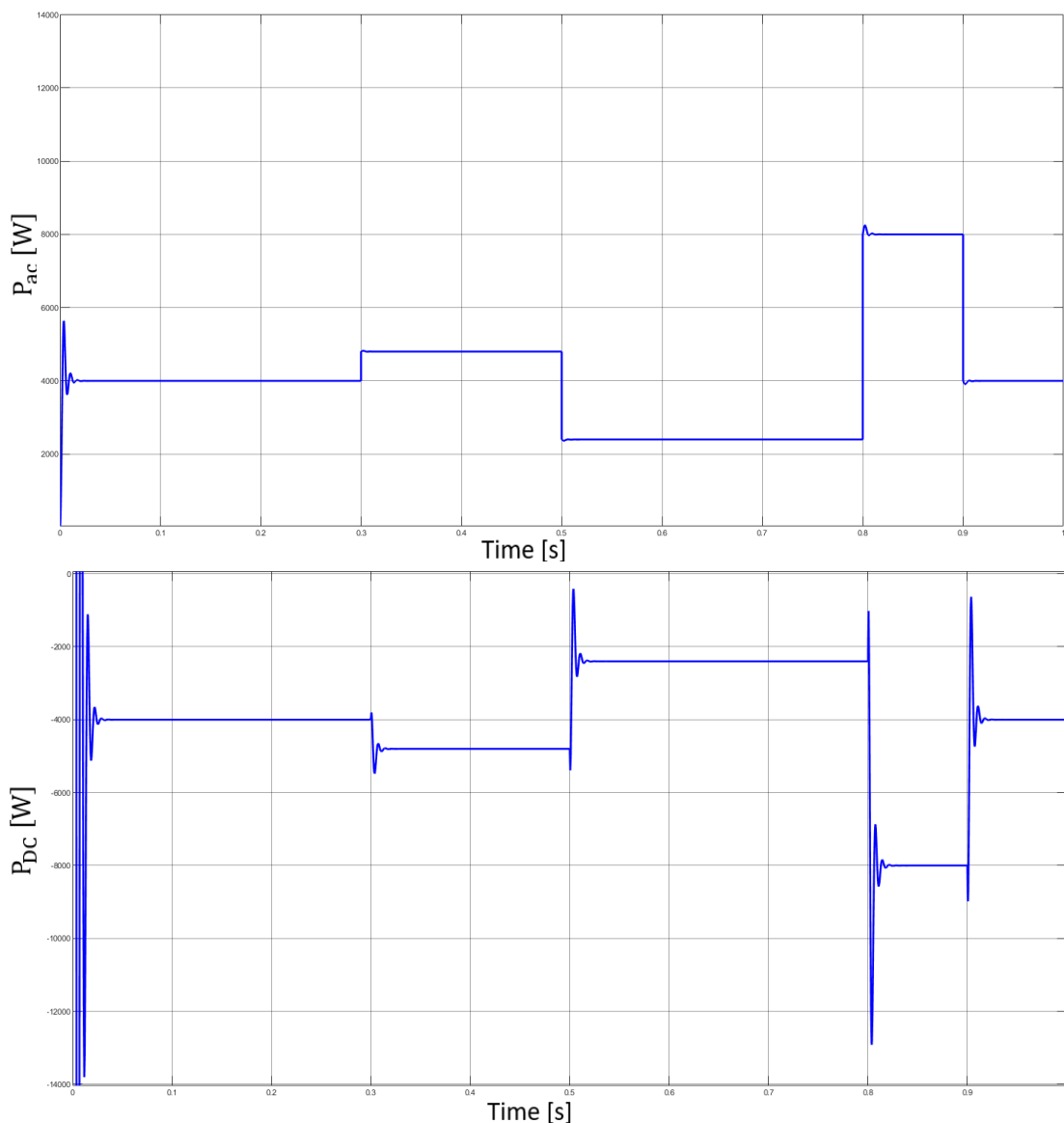


Fig. 27. Signals obtained of  $P_{ac}$ , the plot above, and of  $P_{DC}$ , the plot below.

As can be seen, both active powers are equals in absolute value when the system stabilizes, considering no losses.

## 5. Model of generalized photovoltaic array

In order to simulate a renewable generation system where the external current source is not a particular step but the representation of the power generated by a presumed photovoltaic array, a generalized photovoltaic model is going to be described and implemented with Simulink.

### 5.1. PV array operation

A PV cell has the finality to convert sunlight into electricity. A group of cells form panels or arrays. The principal inputs a PV array has are the cell temperature and the irradiance that it receives, while the external voltage applied to the photovoltaic system would determine the power produced.

The electromagnetic radiation of solar energy can be directly converted to electricity through photovoltaic effect [4]. It is basically a semiconductor diode whose p-n junction is exposed to light [3]. Normally silicon is used to build the cells. Photons with a superior energy than the bandgap of the PV are the only useful, but just the energy equal to the bandgap is used, as the excess will be lost as heat in the PV cell body.

The PV system naturally shows nonlinear  $I$ - $V$  and  $P$ - $V$  characteristics.  $V$  would directly be the external voltage, and  $I$  would basically depend on the radiant intensity and cell temperature. Each specific operating conditions would have concrete  $I$ - $V$  and  $P$ - $V$  curves.

A general scheme of how the photovoltaic system would be adjusted to the converter, which is the purpose of this section, will be presented in Figure 28:

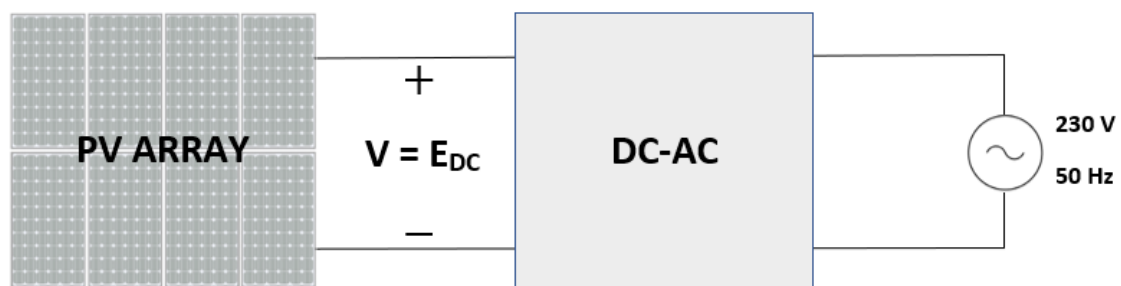


Fig. 28. The general scheme of the PV array connected to the converter, and this connected to the grid.

## 5.2. PV array model

It is going to be used a simplified model [3] that could be implemented in any circuit simulator. Will be represented as a current source and two resistors, as shown in Figure 29:

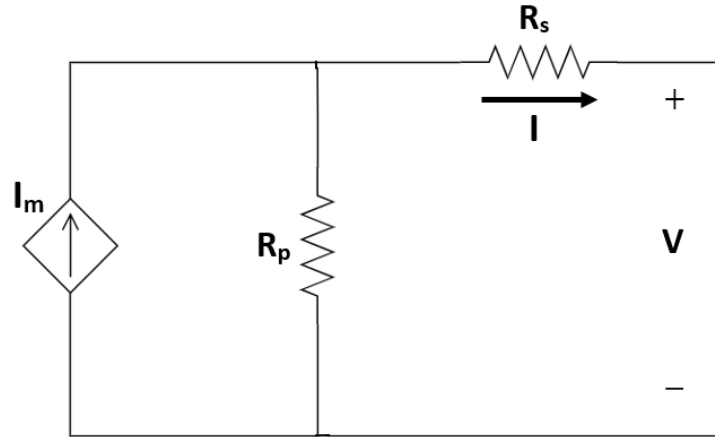


Fig. 29. PV simplified model.

Normally, a diode is included to the photovoltaic models, but in this case the function of the diode is incorporated to the  $I_m$  source, as:

$$I_m = I_{pv} - I_0 \left[ \exp\left(\frac{V + R_s I}{V_t a}\right) - 1 \right] \quad \text{eq. 21.}$$

The second term of this equation corresponds to the diode current, while the first one represents the photovoltaic current. The thermal voltage  $V_t$  depends on how many cells are connected in series as well as on the temperature of the cell.

$$V_t = \frac{N_s k T}{q} \quad \text{eq. 22.}$$

At this point, is going to be expressed how  $I_{pv}$  and  $I_0$  can be obtained.

The light-generated current of the PV,  $I_{pv}$ , depends on the temperature and the solar irradiation captured by the plate. The following equation is used:

$$I_{pv} = [I_{pv,n} + K_I(T - T_n)] \frac{G}{G_n} \quad \text{eq. 23.}$$

The diode saturation current  $I_0$  would also depend on the temperature. It can be expressed as:

$$I_0 = I_{0,n} \left(\frac{T_n}{T}\right)^3 \exp\left[\frac{qE_g}{ak} \left(\frac{1}{T_n} - \frac{1}{T}\right)\right] \quad \text{eq. 24.}$$

With these four equations and the parameters of an adjusted model of the KC200GT solar array, considering an actual state of  $T=25\text{ }^{\circ}\text{C}$  and  $G=1000\text{ W/m}^2$ , the following parameters listed in Table 3 will be used to determine the whole model [3]:

$I_{pv,n}$	8,214 A	$k$	$1,380649 \cdot 10^{-23}\text{ J/K}$
$I_{0,n}$	$9,825 \cdot 10^{-3}\text{ A}$	$R_p$	415,405 $\Omega$
$N_s$	54	$R_s$	0,221 $\Omega$
$T_n$	298,15 K	$a$	1,3
$T$	298,15 K	$q$	$1,602176634 \cdot 10^{-19}\text{ C}$
$G$	1000 $\text{W/m}^2$	$E_g$	1,12 eV
$G_n$	1000 $\text{W/m}^2$	$K_I$	0,0032 A/K

Table 3. Parameters of the adjusted model of the KC200GT solar array. A silicon cell at  $25^{\circ}\text{C}$  and a  $1000\text{ W/m}^2$  irradiation has been considered. [3]

### 5.2.1. PV array connected to a DC voltage source

First, before connecting the photovoltaic system to the converter, a study with a DC voltage source is going to be done in order to analyze the behavior of the system. A power converter of 10 kVA of apparent power with a DC bus voltage reference of 800 V was considered, so the peak of the  $P$ - $V$  curve of the array should be close to the  $P=10.000\text{ W}$  and  $V=800\text{ V}$ . The PV array model should be adjusted to this comportment so it could be connected with the VSC further on. At first, the simple model presented in Figure 29 connected to a voltage source will be analyzed to ensure a correctly behavior of the model.

To make this first simulation, the following model shown in Figure 30 will be used:

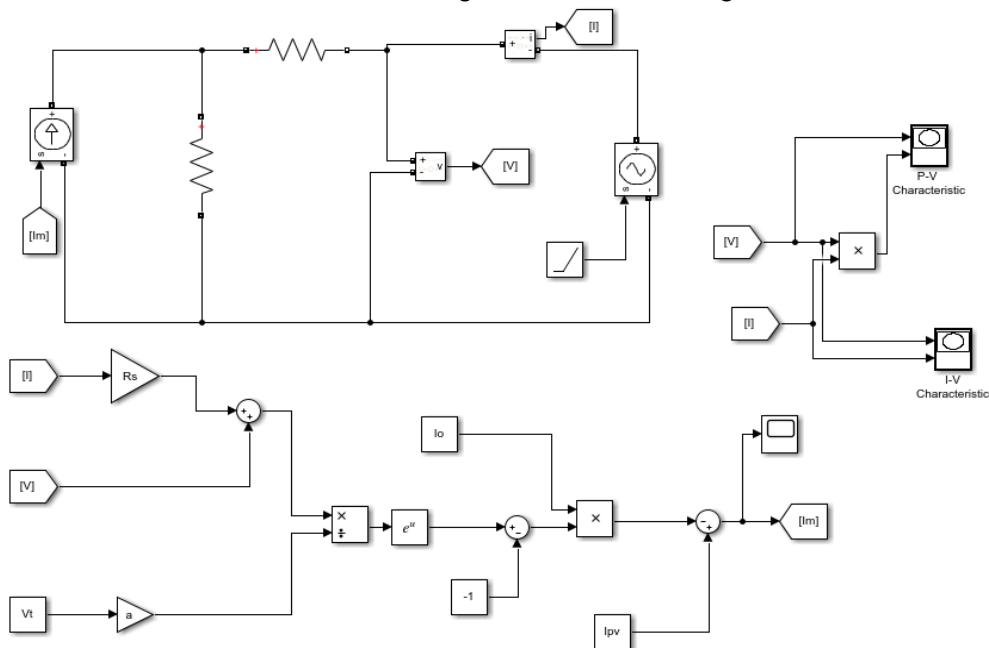
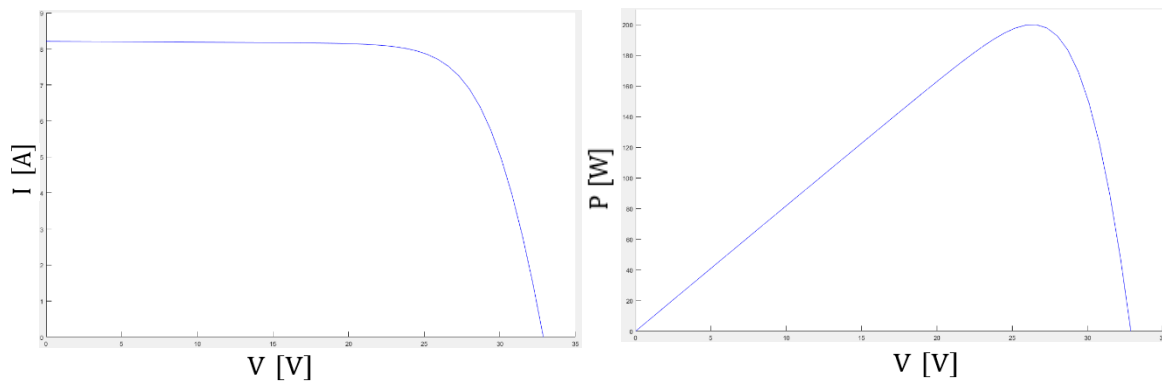


Fig. 30. PV array model connected to a DC voltage source.

Equations 21, 22 and 23 were implemented to the Matlab Workspace, as none of those are related to the variables  $I$  or  $V$ . A ramp with a slope of 35 V/s will be used to define the DC voltage source. With the model and the source established, the following  $P$ - $V$  and  $I$ - $V$  curves were obtained:



**Fig. 31.**  $I$ - $V$  plot on the left,  $P$ - $V$  plot on the right. Extracted from the PV array connected to a DC voltage source simulation.

A maximum power peak is obtained when  $V=26,53$  V with a power of 200 W. Obviously, the results shown in Figure 31 are far from the power converter behavior, so some adjustments must be made later on.

To get an initial idea of how the system can evolve by changes in the sunlight, it is going to analyze the differences in the behavior of the panel when multiple values of irradiation and temperature are used. It is going to part from the so-called *standard test conditions* (STC), which correspond to a temperature  $T=25^{\circ}\text{C}$  and an irradiation of  $G=1000$  W/m<sup>2</sup>. The previous curves have been obtained with these conditions.

First, changes on the temperature with a constant STC irradiation will be implemented:

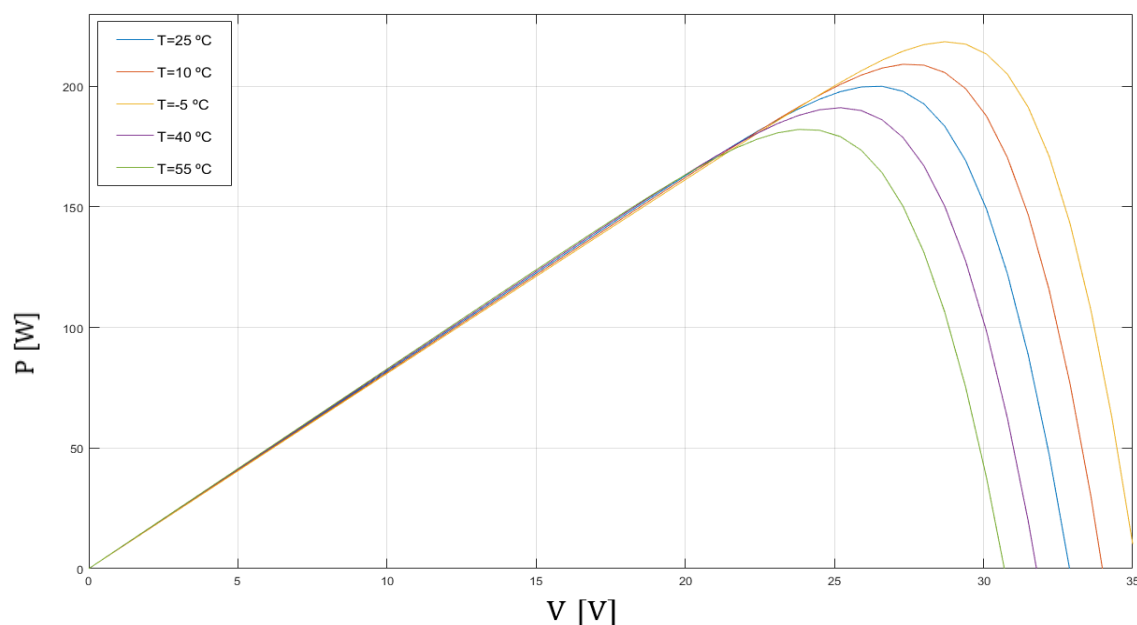


**Fig. 32.** Plot of  $P$ - $V$  curves for different temperature values.

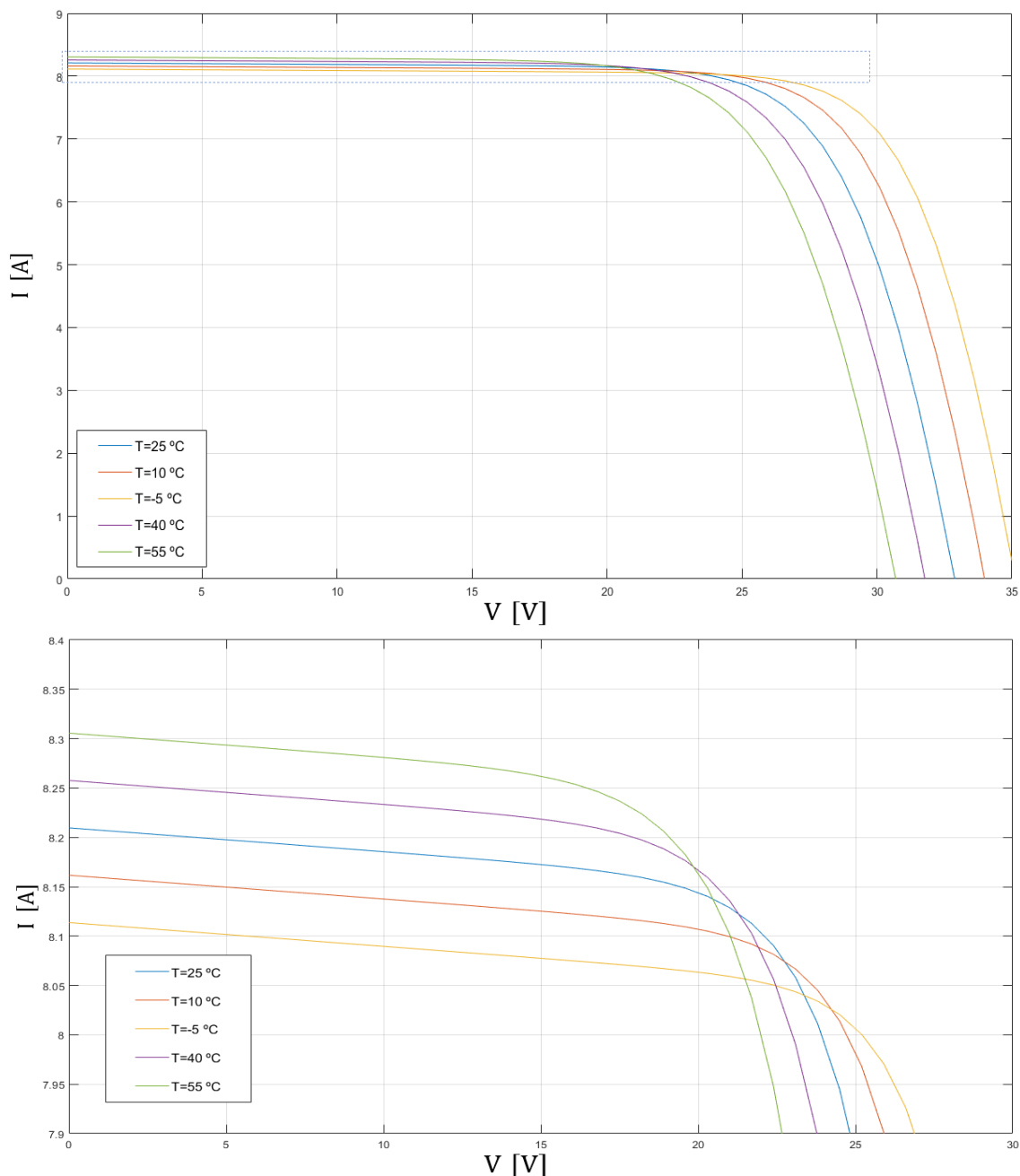


**Fig. 33. Plots of  $I$ - $V$  curves for different temperature values. Plot on the top is the general curves, plot on the bottom is a zoom of a zone of interest.**

It is appreciable in both figures 32 and 33 how a higher temperature leads to an increase in the maximum current, whereas the maximum power decreases. That's because the point where the current starts to decrease drastically occurs in a lower voltage while the temperature is diminished. As the increase of current is lower than the decrease of voltage in absolute value, the power is reduced. So, there is a reduction in the maximum power, which occurs in a lower voltage each time temperature is decreased. The point where maximum power is obtained is called *maximum power point* (MPP), which happens in  $V_{mp}$  and  $I_{mp}$ .

Something similar happens when changes in solar irradiance are introduced while the temperature is fixed in STC.

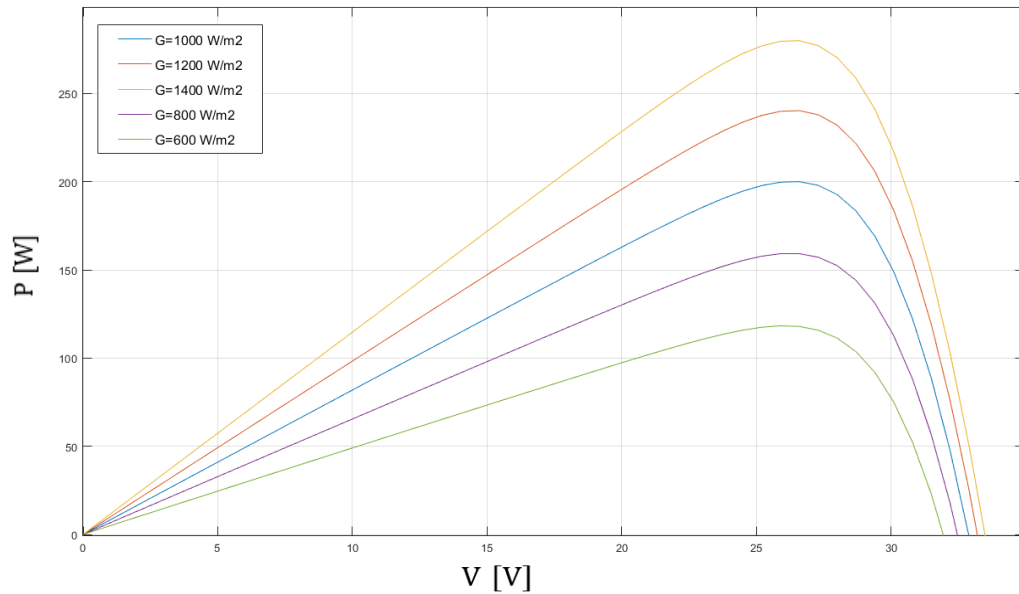


Fig. 34. Plot of  $P$ - $V$  curves for different irradiation values.

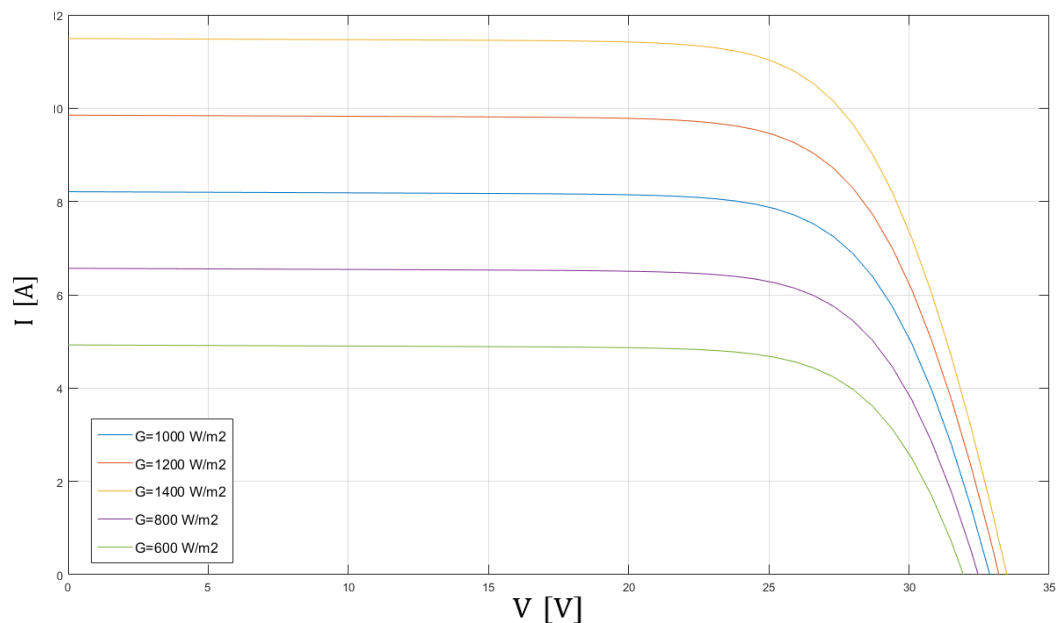


Fig. 35. Plot of  $I$ - $V$  curves for different irradiance values.

In this case, when higher solar irradiation is received, there is an increase of current and a slight rise of  $V_{mp}$  voltage, as can be seen in Figures 34 and 35. In consequence, higher powers will be obtained practically at the same voltage. The reason why the system has this behavior when changes in irradiance are applied would be because open-circuit voltage is logarithmically dependent on the solar irradiance, while short-circuit current is directly proportional to irradiation.

Summing up:





### 5.2.2. Adaptation of the PV model

As the presented PV array produces very low power compared with the power the VSC works with, a new variety of PV model would be used to try to reach the 10 kW at 800 V peak. A new configuration considering cells connected in series and in parallel will be arranged. After all, a PV array is a group of PV modules connected in series and parallel circuit design to produce the required power [5]. With the new configuration, where the series cells  $N_s$  and parallel cells  $N_p$  are considered, a new but similar simplified PV model will be needed, showed in Figure 36:

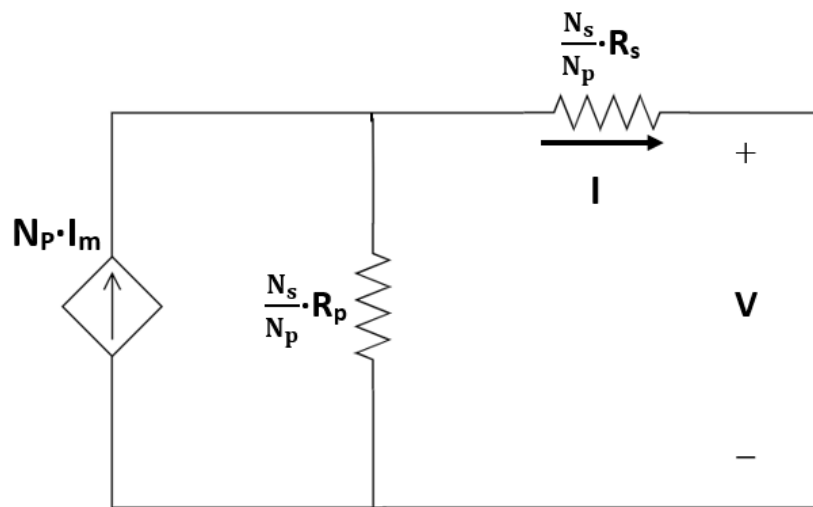


Fig. 36. PV simplified model considering series and parallel connected cells. [4]

With this new model, a new equation will be applied to control find the model current:

$$N_p I_m = N_p I_{pv} - N_p I_0 \left[ \exp \left( \frac{q \left( \frac{V}{N_s} + \frac{I R_s}{N_p} \right)}{V_t \alpha} \right) - 1 \right] \quad \text{eq. 25.}$$

As the cells connected in parallel increase the current and cells connected in series provide greater voltage outputs, those values will have to be modified to try to reach the mentioned peak.

A slope of 1000 V/s will be used to define the DC voltage source, as the  $V_{mp}$  voltage will be forced to be at 800 V. Therefore, the same KC200GT panel will be considered, using the parameters of Table 3. With these conditions, to obtain a maximum power of 10 kW at 800 V, will be needed  $N_s = 30$  cells connected in series and  $N_p = 1,65$  in parallel. Obviously, those values are not achievable, but with the parameters of this concrete solar array it is not possible to reach the expected MPP with integers.

By the way, the mentioned  $N_s$  and  $N_p$  values are going to be used, although it is known that, in a real system, a panel with other parameters should be used to reach the desired power in the desired voltage.

With the mentioned parameters and number of cells, the following  $P$ - $V$  and  $I$ - $V$  curves shown in Figure 37 will be obtained:

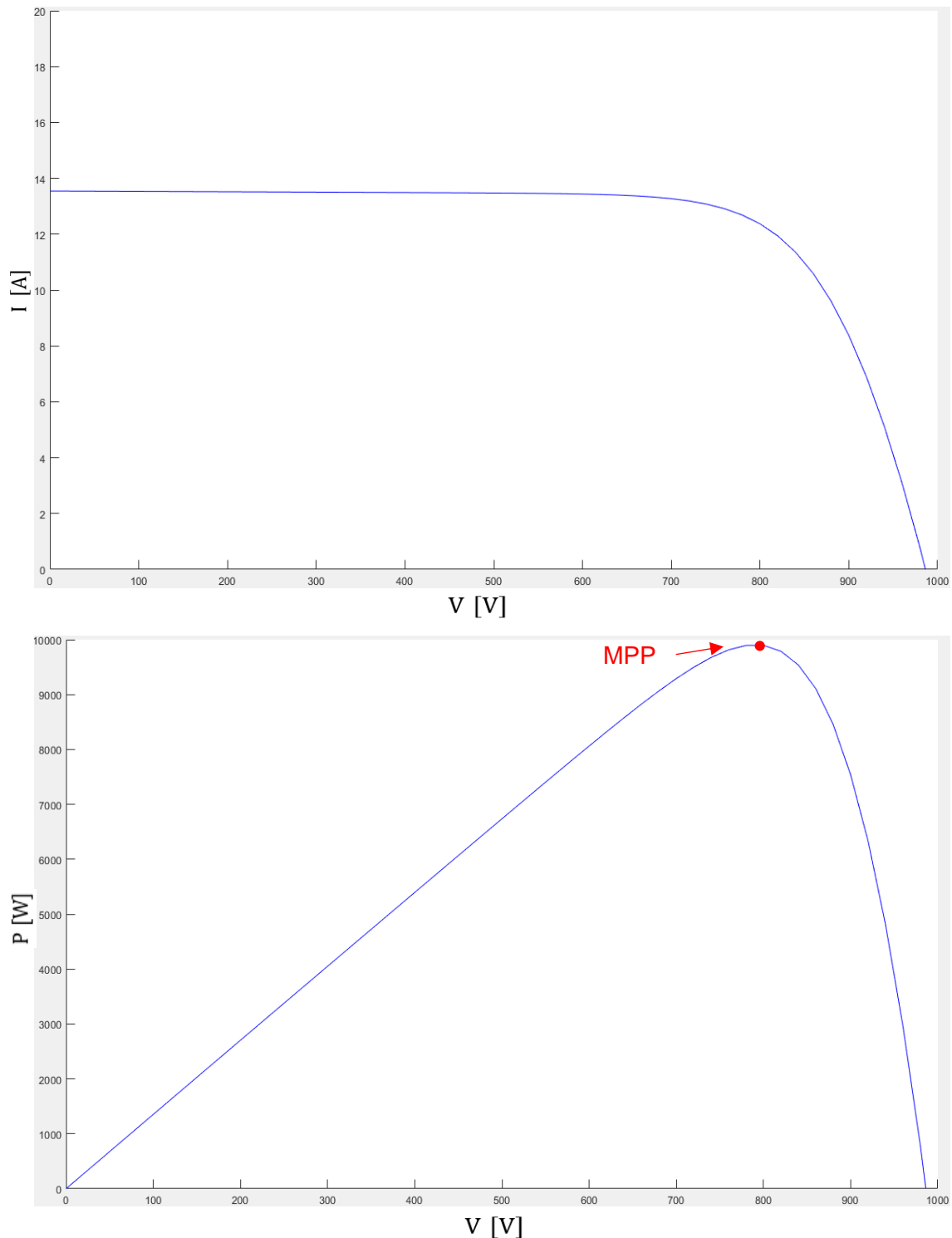


**Fig. 37.**  $I$ - $V$  plot on the top,  $P$ - $V$  plot on the bottom. Extracted from the adapted PV array connected to a DC voltage source simulation.

A power of 9.895 W is achieved at a voltage of 800 V. This point is very close to the MPP, so the model is accepted to be implemented with the converter.



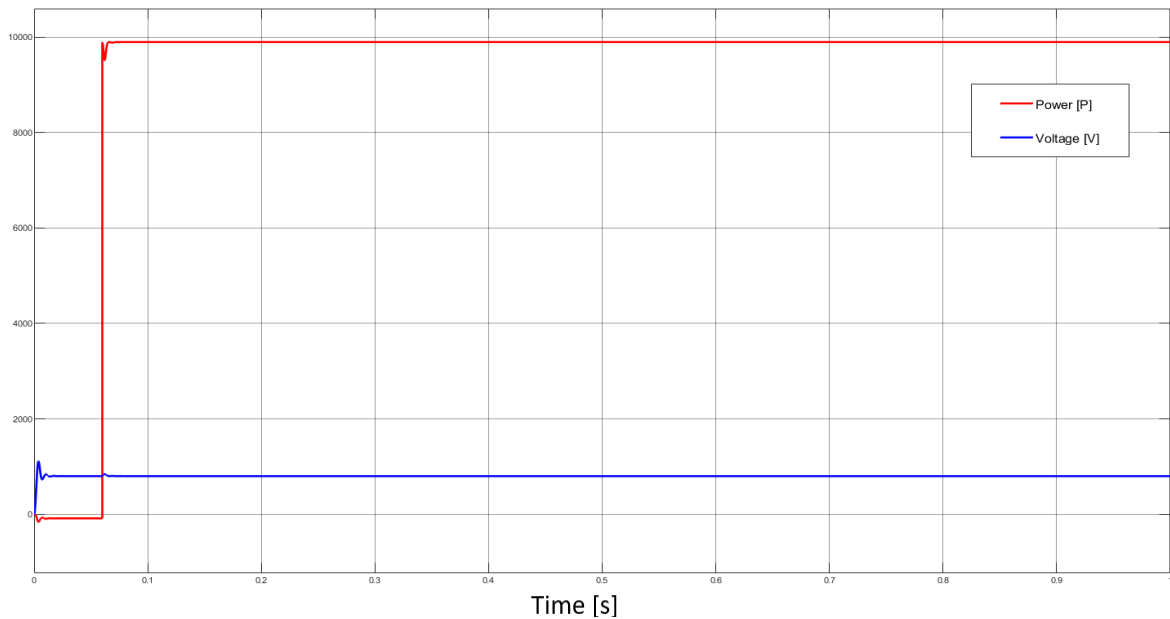


Fig. 39. Plot of the power injected to the system and the  $E_{DC}$  voltage

The voltage remains tending to the reference value of  $E_{DC}^* = 800$  V due to the DC voltage regulator. Can be seen in Figure 39 that in  $t=0,06$  s, when  $I_m$  starts to be different from zero, the power turns into the expected constant value of nearly 10 kW.

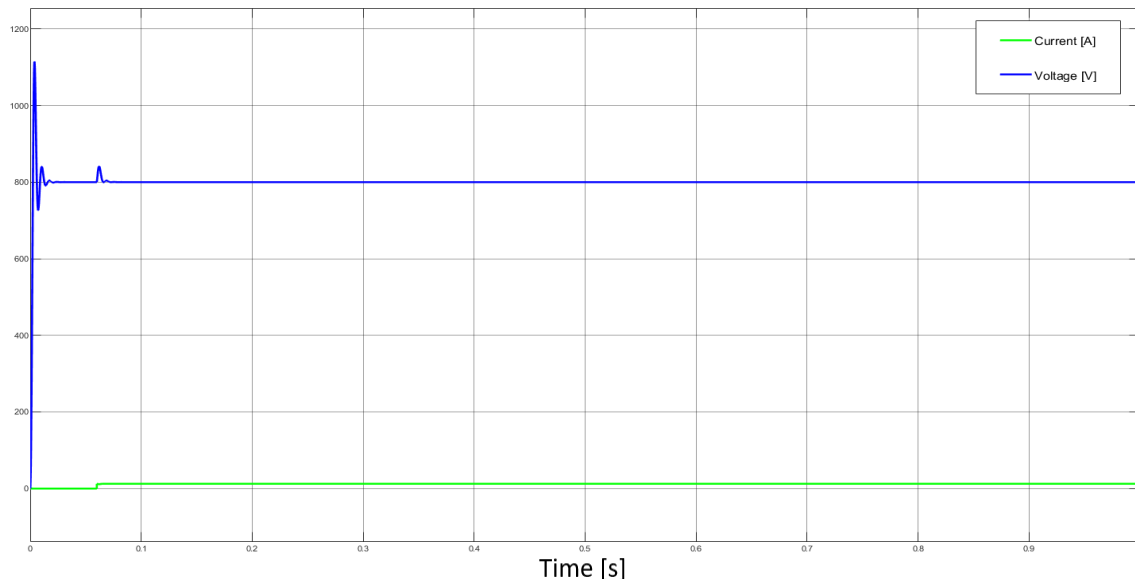


Fig. 40. Plot of the current injected to the system and the  $E_{DC}$  voltage

The current achieved in the adapted model in the 800 V is also reached here, as can be seen in Figure 40, which remains constant as the power, at  $I_{DCm}=12,37$  A. So, the objective of the adapted model is achieved as the expected behavior is reached.

### 5.3. Maximum power point tracking (MPPT)

The maximum power point tracking (MPPT) is an algorithm used in PV inverters to continuously adjust the impedance seen by the solar array to maximize the power extraction although some conditions as irradiance or temperature could change. The intention will be to adjust the voltage reference  $E_{DC}^*$  to provide the required DC bus voltage that would maximize the energy provided.

#### 5.3.1. Presentation of the MPPT algorithm

The three most common MPPT algorithms used to achieve the maximum power are:

- **Perturbation and observation (P&O).**
- Incremental conductance.
- Fractional open-circuit voltage.

The first algorithm is going to be implemented, exposed in Figure 41:

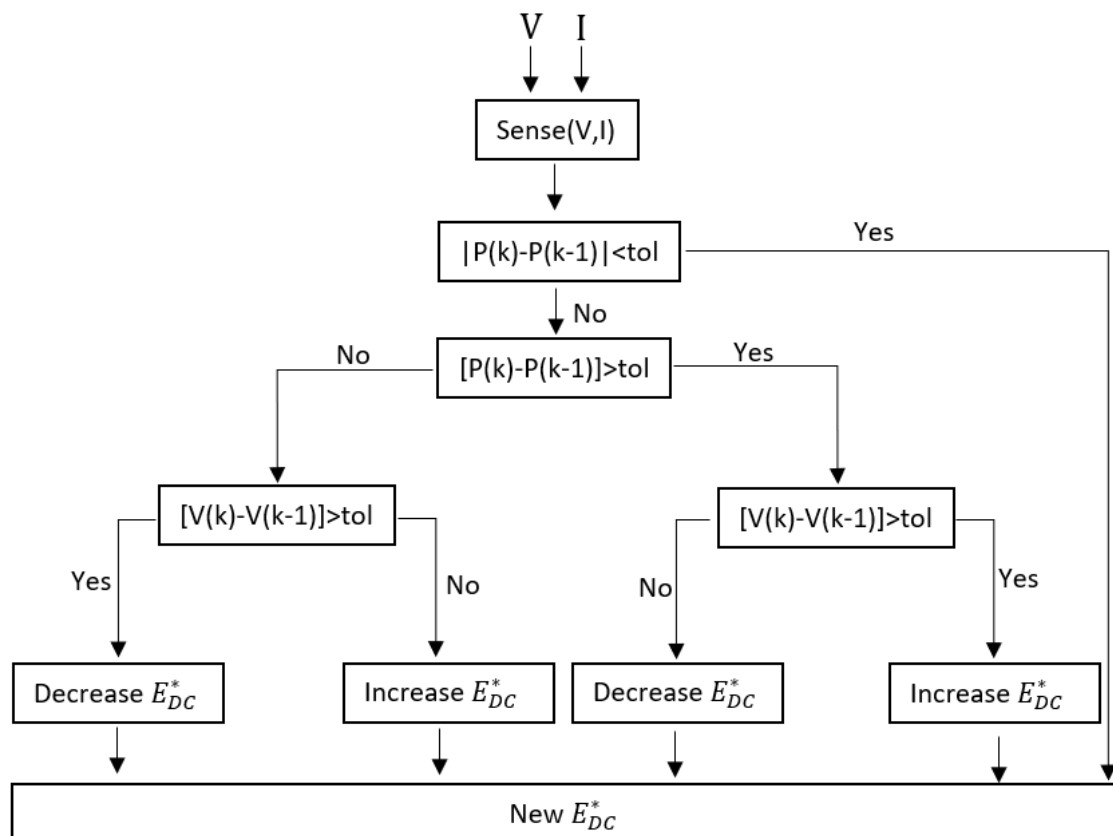


Fig. 41. MPPT algorithm used. Based on [6].

This kind of perturbation and observation algorithm is used by implementing a Matlab function. First, the power is calculated with DC bus voltage and current measures. In the first execution of the function, some initial values of power, voltage, and voltage reference must be imposed. Those are necessary to compare the actual  $k$  variables with their respective previous  $k-1$ , which in the first iteration don't exist. Some specific aspects should be taken in count:

- It is important to choose a coherent value for the **initial voltage reference**. Through the iterations, this initial value would be increased or decreased in order to achieve the MPP voltage, and maybe the system wouldn't do enough iterations through the simulation to reach it, so a close value to the expected  $V_{mp}$  should be taken. As seen previously, a voltage reference close to 800 V is expected when STC conditions are present, so, in this case, an initial voltage reference of **800 V** will be chosen to help the software to reach the optimum voltage. Initial voltage and power should be also determined, but those chosen values don't affect the development of the simulation.
- The same happens with the  $\Delta V$ . This magnitude represents how much the reference voltage would be enlarged or reduced. If, for example, in each iteration, the magnitude changes in 10 V, it is highly probable that  $E_{DC}^*$  would never coincide with  $V_{mp}$ , so the reference voltage will be oscillating without reaching the desired value. Otherwise, is it probable that if this number is too short, the system wouldn't do enough iterations to achieve the value, similar to the previous case. After observing the behavior of the system using different values,  $\Delta V = 0,02 \text{ V}$  will be used in STC.
- The value of **tolerance**  $tol$  is also important. If the tolerance is too short, maybe the system considers two powers or voltages as different when it should treat them as equals. On the other hand, if too high tolerance is imposed, the opposite would happen, considering equals two different values. A tolerance value of  **$tol = 0.01$**  will be used, as it seems to give a correct comportment of the system in STC.
- It is needed to adjust the **sampling time** value of the function block. In the same direction as the other aspects, enough little *sampling time* value is needed to ensure the system would reach the optimum voltage. A setting of  $1 \cdot 10^{-5} \text{ s}$  has been chosen at first.

### 5.3.2. VSC connected to the PV array with MPPT

Once the whole system is defined, different studies are going to be made:

- Stabilization of the system in standard conditions ( $T=25^{\circ}\text{C}$ ,  $G=1000\text{ W/m}^2$ ).
- Evolution of the system with a constant temperature and a changing irradiation.
- Evolution of the system with a constant irradiation and a changing temperature.

At first, it is going to see if the algorithm works properly by analyzing how the DC voltage reference changes until it gets stabilized into the  $V_{mp}$  in the standard conditions STC. The evolution of  $E_{DC}^*$  will be seen in the following figure:

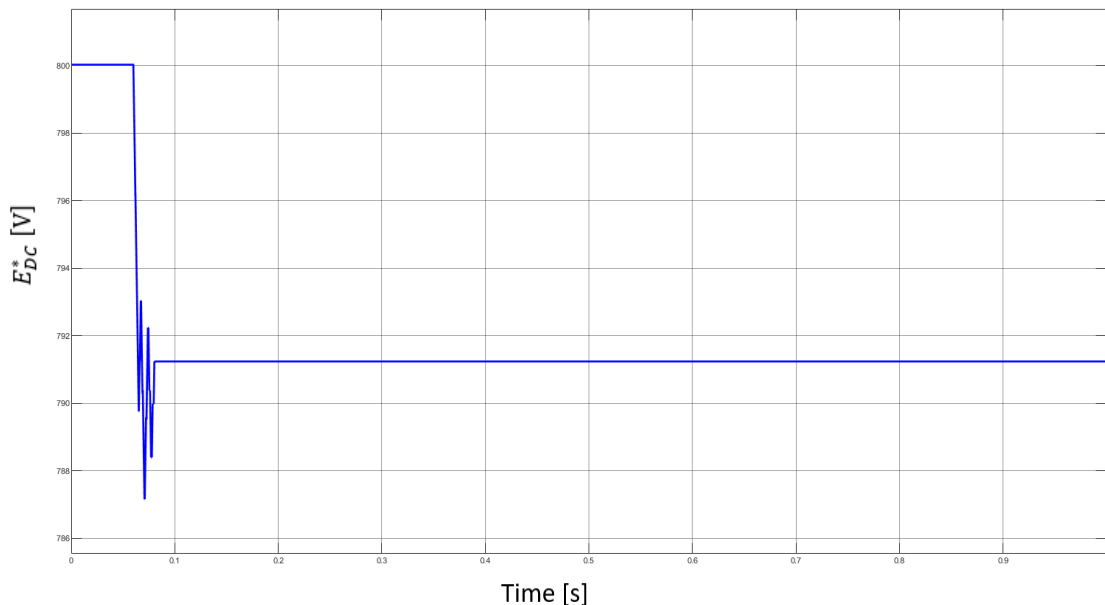


**Fig. 42. Plot of the DC voltage reference.**

As can be seen in Figure 42, the voltage reference starts at the imposed initial value of 800 V. When the current starts to change, at  $t=0,06\text{s}$ , the power begins to be different from zero and the function tries to reach the  $V_{mp}$  value. In this case, the optimum DC bus voltage reference is established at 791,2 V, close to the 800 V that were tried to reach with the adapted PV array model. With this voltage, the following power is obtained:

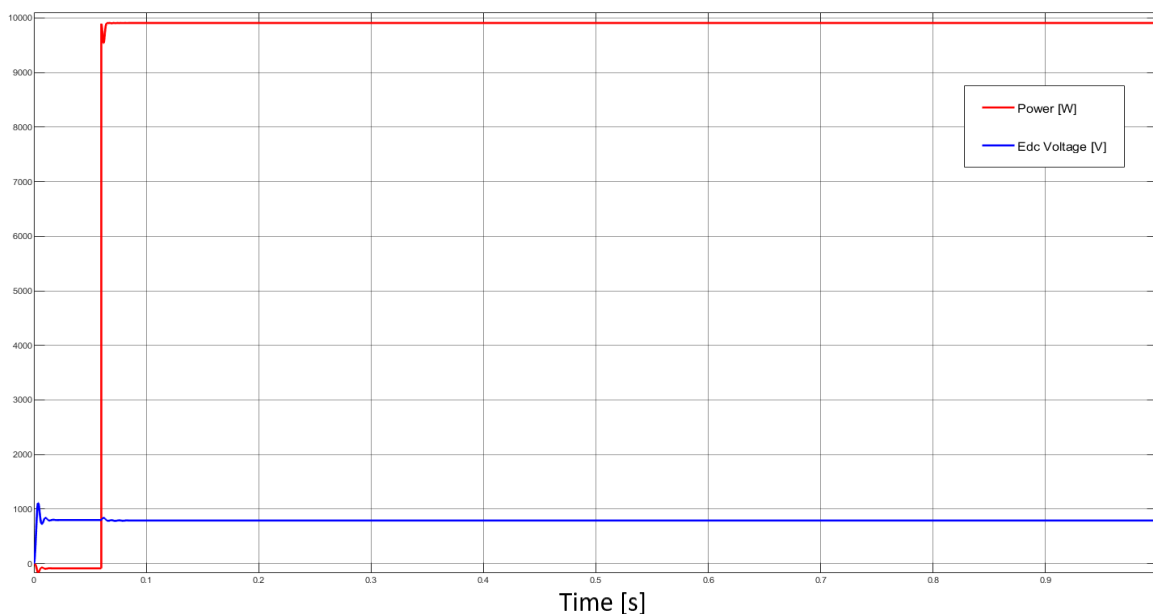


**Fig. 43.** Plot of the power injected to the system and the  $E_{DC}$  voltage.

This plot, presented in Figure 43, seems to be the same as the one in Figure 39, but while in the previous case the DC bus voltage was following the constant  $E_{DC}^* = 800$  V, in this simulation the voltage tends to be the optimum bus voltage reference obtained with the MPPT. With the  $V_{mp}$  value of 791,2 V, a power of 9.907 W is reached. Thus, the values intended with the adapted model can be assumed as accepted.

To see the evolution when changes in irradiance or temperature are imposed, the previous equations 22, 23 and 24 will be needed in the model to input them in equation 21, as in the workspace is not possible to change its value during the simulation. The simulated model is showed in Figure 44. To express the variation of temperature, ramps will be used, while with irradiance some steps will be implemented to compare the behavior. That's because the gradient of temperature is expected to be slower than the gradient of irradiance.



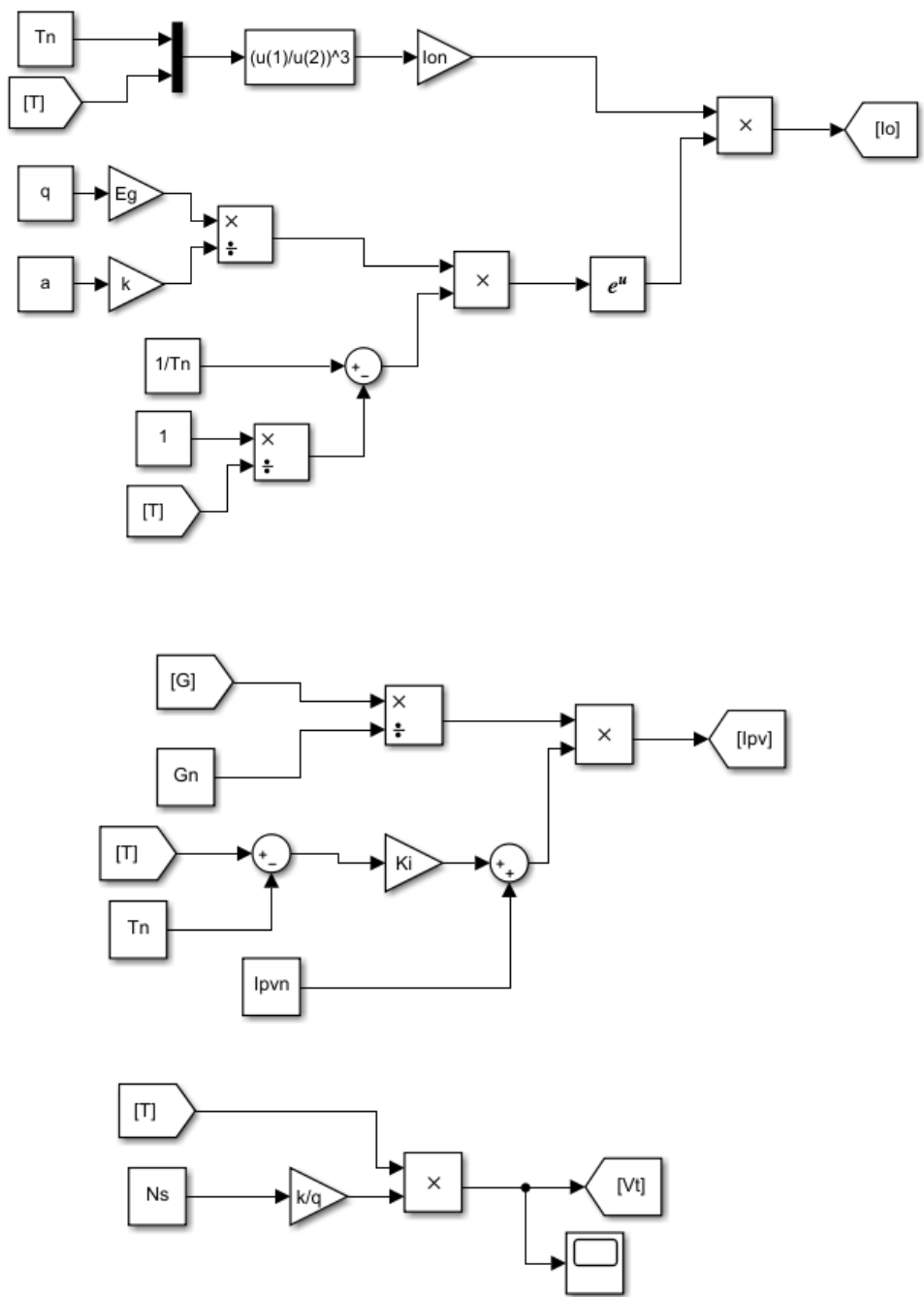


Fig. 44. The first represents eq. 24, the second eq. 23 and the third equation 22.

When changes in the irradiance are applied while the temperature remains constant at 25°C, the MPPT would make the system constantly regulate the voltage reference to obtain the maximum possible power. The following simulation has been done with  $t_{ol}=1\cdot 10^{-4}$ ,  $\Delta V=0,002$  V, an initial voltage reference of 750 V and a sampling time of  $1\cdot 10^{-5}$ s.

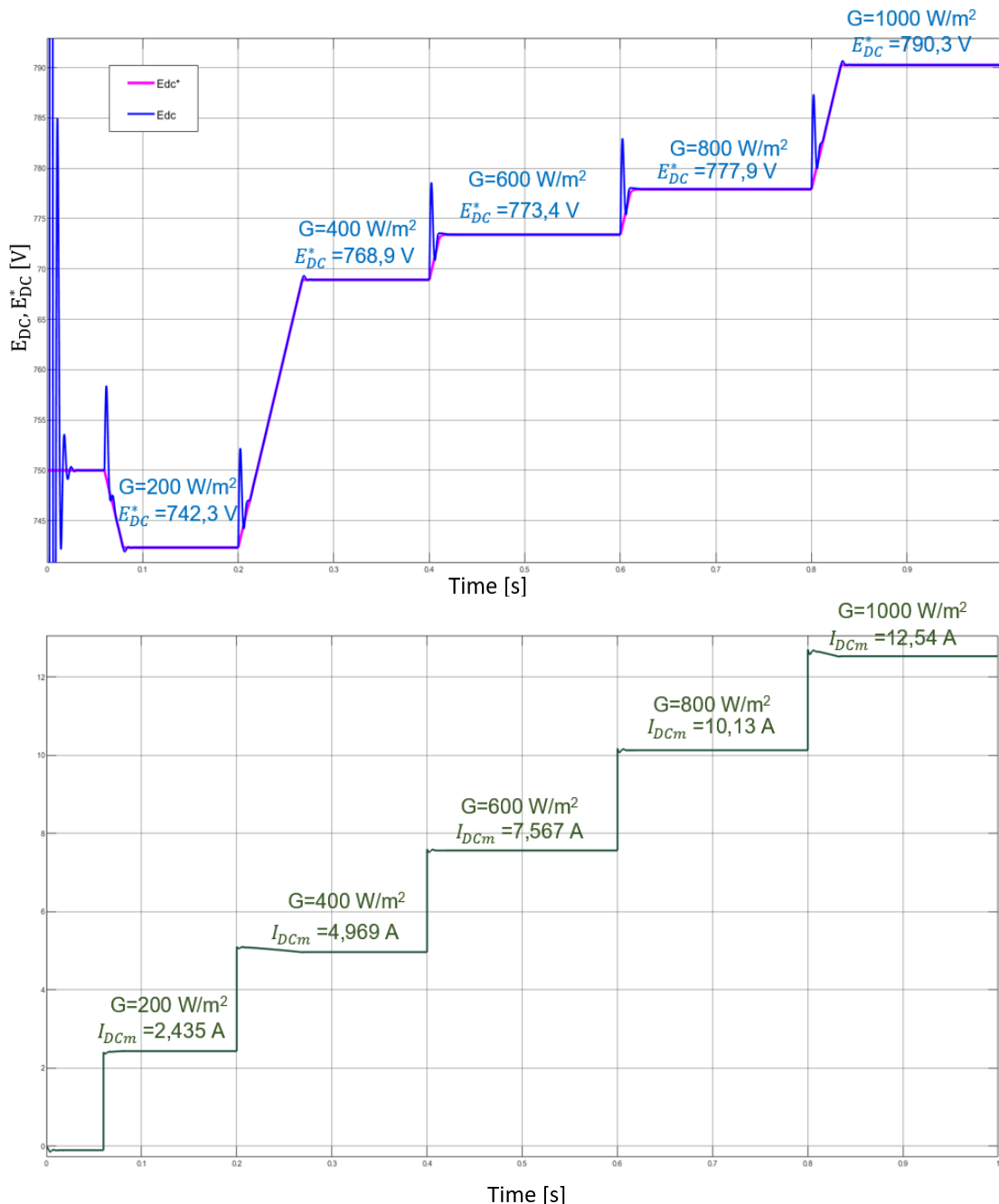


Fig. 45. Simulation with constant temperature and changing irradiance. On top, plot of real and reference voltage. On bottom, plot of the current injected to the grid.

As can be seen in Figure 45, in the periods voltage is increasing, current is also decreasing a little bit, so the power remains practically constant while the irradiation is constant. This can be seen in Figure 46:

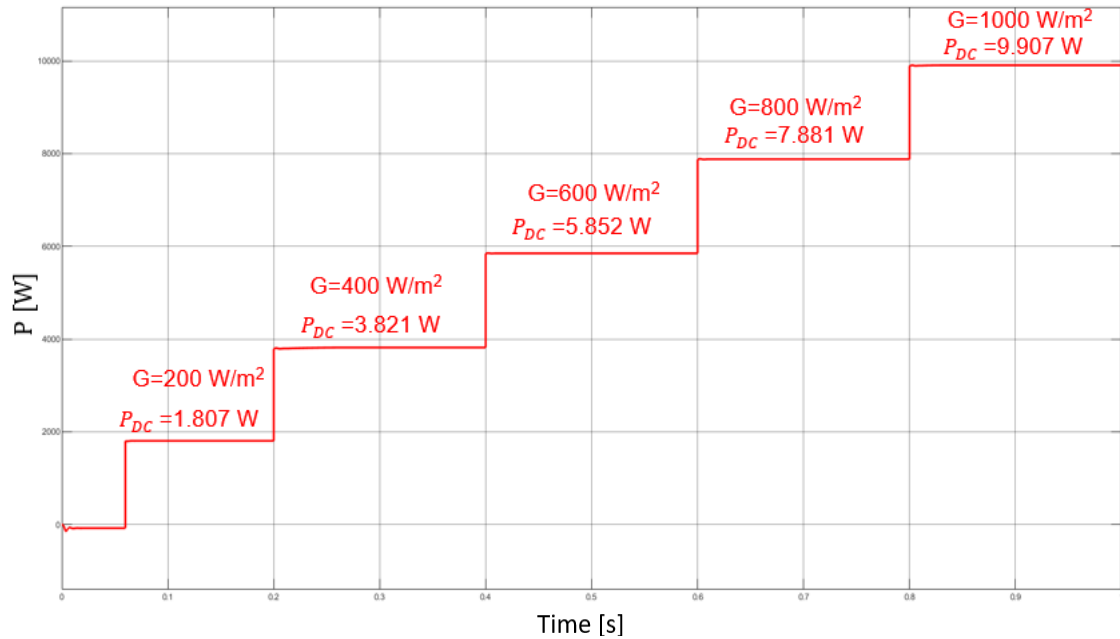
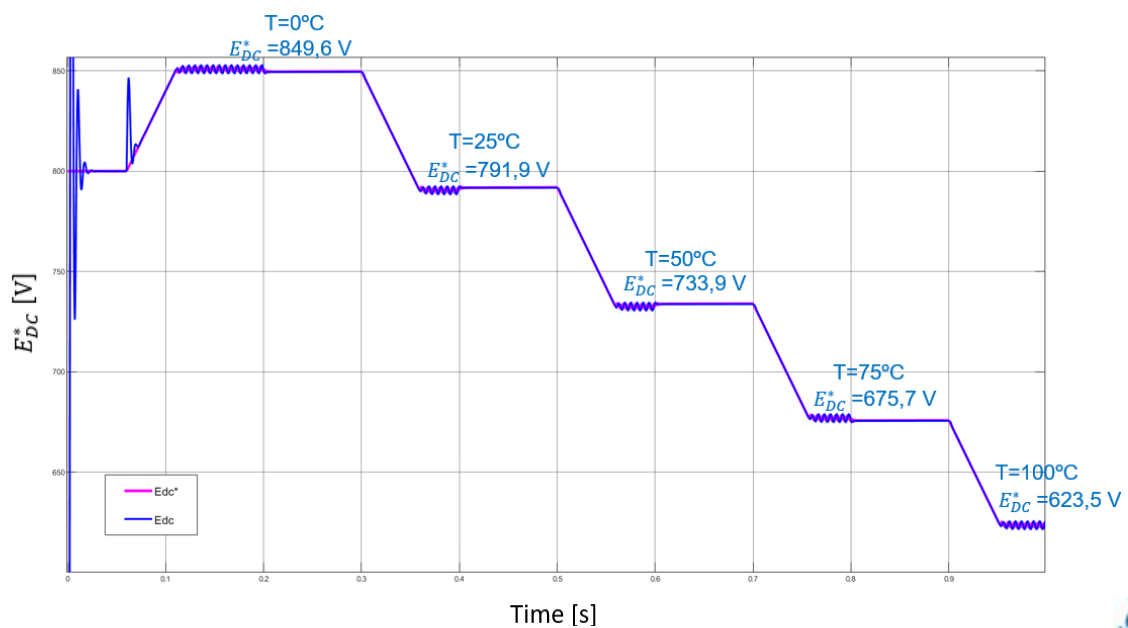
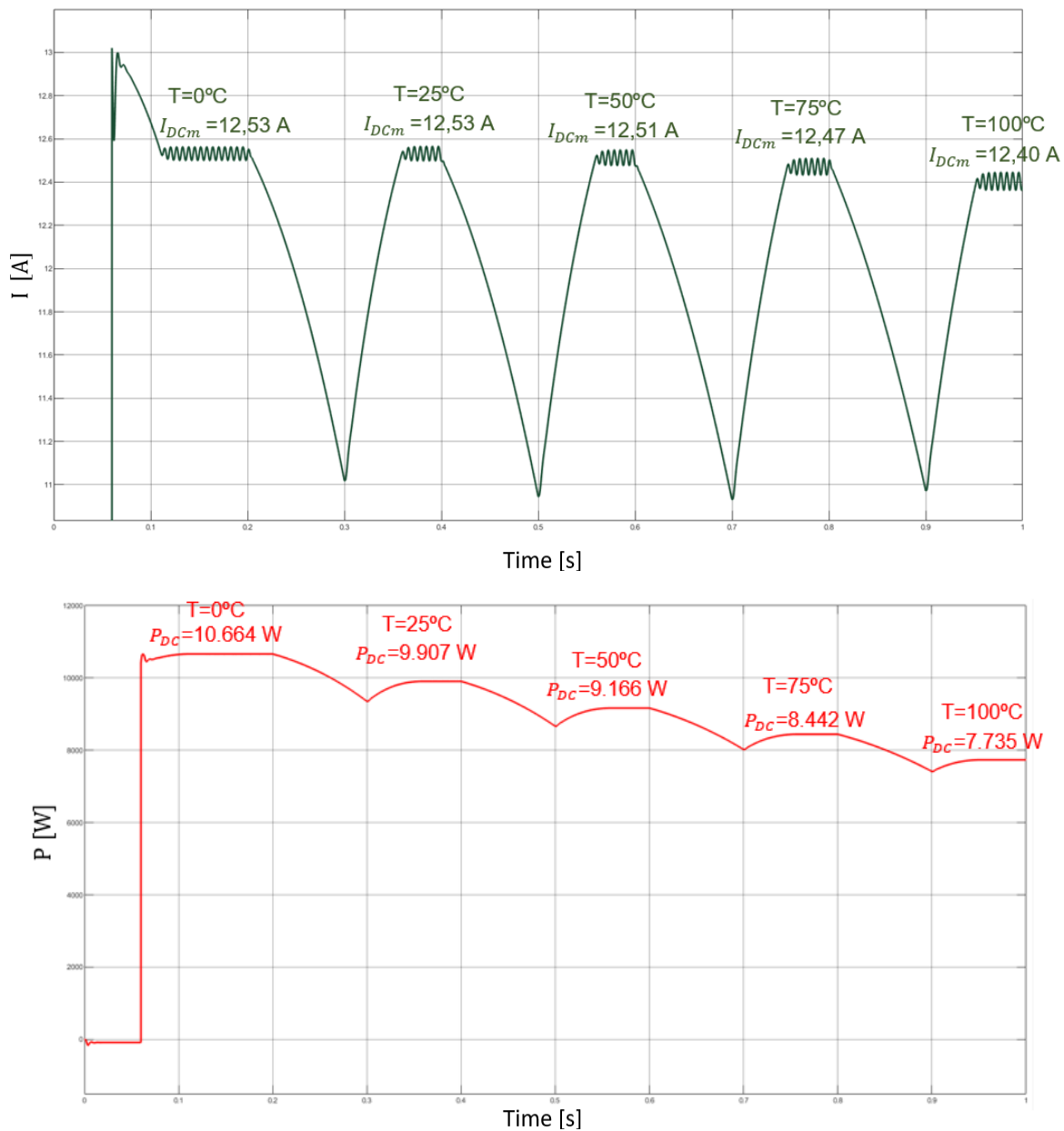


Fig. 46. Power plot of the simulation with constant temperature and changing irradiance.

It is appreciable how the maximum possible power is reached by adapting the voltage reference. Something similar will be done fixing an irradiance of  $1000 \text{ W/m}^2$  and changing the value of temperature. In this simulation, a major variance of voltage is going to be seen, so to ensure the system could reach the expecting values new function parameters are used: a tolerance  $tol=0$ , a voltage reference variation  $\Delta V = 0,005 \text{ V}$ , an initial voltage reference of  $800 \text{ V}$  and a sampling time of  $1 \cdot 10^{-6} \text{ s}$ . That's why there are some oscillations in the plot showed at Figure 47, as with this  $\Delta V$  the exact  $V_{mp}$  value is difficult to reach, but is needed to, at least, get as close as possible to it. The current values showed are the average current of the oscillation.





**Fig. 47. Simulation with constant irradiance and changing temperature. The first plot corresponds to real and reference voltage. The second, to the injected current to the grid. Third, plot of the power injected to the grid.**

The difference in the shape with this curves and the ones presented in Figures 45 and 46 is due to the usage of ramps instead of steps. It is like the MPPT waits until the temperature is stabilized to start changing the voltage reference to reach the  $V_{mp}$  value. To study this fact, the simulation period from 0,2s to 0,4s will be used, dividing it in two parts:

1. From 0,2s to 0,3s, temperature changes from  $0^\circ\text{C}$  to  $25^\circ\text{C}$  by a ramp.
2. From 0,3s to 0,4s, temperature is constant on  $25^\circ\text{C}$ .

To make the explanation clearer, the  $I$ - $V$  and  $P$ - $V$  plots of both temperatures will be used in Figure 48:

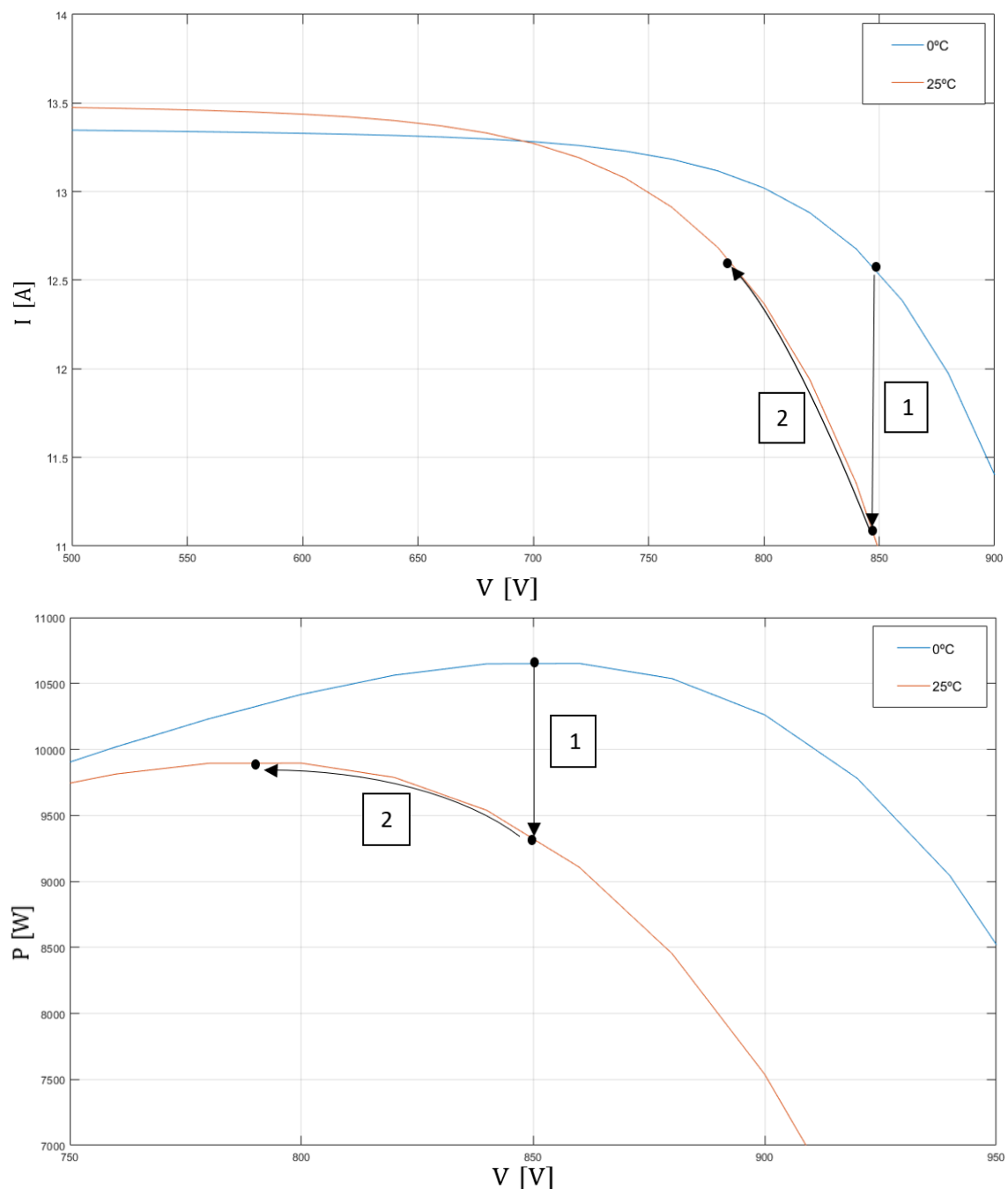


**Fig. 48. Simulation with STC irradiance and  $0^\circ\text{C}$  and  $25^\circ\text{C}$  temperatures. On top, plot  $I$ - $V$  curves. On bottom, plot of the  $P$ - $V$  curves.**

As can be seen, in period 1, from 0,2s to 0,3s, the voltage remains constant while the system is moving from one curve to the other, decreasing its current and power. Then, in the second period, from 0,3s to 0,4s, the system tries to reach the  $V_{mp}$  value of the respective curve, increasing both current and power until it achieves the optimum power. Once it is reached, the voltage reference starts to oscillate around that value due to the parameters imposed, until a new change of temperature is applied.

In fact, a gradient of 25°C in 0,1s never occur, but it is interesting to see how the system would react, so this kind of comportment won't be seen in reality.

In both studies, it is able to see how a higher power is obtained by increasing the irradiance with a constant temperature, whereas with a higher temperature and a constant irradiance the power decreases, as presented in section 5.2.1.. The optimum power is reached in each situation adapting the voltage to its optimum value.

## 6. Environmental Impact

Considering this project such as a model of an overall photovoltaic system, the environmental effects are not significant, as only the impact would be the caused by the electricity consumed by the computer.

By the way, a way of converting renewable source into electricity is studied through the project, so it has an indirect positive impact on the environment. This project could be useful to understand the working of the whole system to try to implement a real PV array with the respective converter. It is known that renewable sources need to take the spotlight to make the world cleaner, but some points must be considered.

First, the process of producing and installing the system has to be considered. Energy is needed to fabricate the array and the converter. Supposing that this energy is coming from a non-renewable source, it is worthy to be used, as a big reduction of polluting emissions will be achieved. Then, installing the system means to alter the terrain where it is implemented, although if the array is not very big it can be installed practically everywhere in comparison with other renewable sources.

However, recycling the PV systems is quite efficient, as the panels can be almost completely recycled (85-90%). So, knowing the pollution generated by the energy provided by the PV array is negligible compared with the greenhouse effect induced by the non-renewable sources, the only drawback to installing solar panels is their high price.

In summary, the project based on the simulated model does not have any kind of significant environmental impact, but if it were useful to provide the knowledge to implant a real PV system, it would have real positive effects, as it would lead to a reduction in pollutant emissions.

## 7. Economic Study

Taking into consideration the project started from scratch, the following items used to develop the project with the respective price have been taken into account:

Item	Cost	Units	Total [€]
Computer	1.300 €	1	1.300 €
Matlab and Simulink student suite license	69 €	1	69 €
Simscape Electrical extension	69 €	1	69 €
Microsoft office	70 €	1	70 €
Engineer salary	20 €/h	250 h	5.000 €
Total		6.508 €	

**Table 4. Economic analysis of the project costs.**

It is remarkable to say that this project was done from February 2020 to June 2020. Some of the values used in Table 4 are approximations, as the price of the computer and the salary have been introduced considering a fair price. The exact number of hours invested in this project have not been counted at all, but 250 h must be near to the real time spent in. So, the total cost of the project would be 6.508 €.



## 8. Conclusions

After all the studies done, it has been able to appreciate the relevance of engineering in the process of obtaining renewable energy. It is an essential complex process that would have to be implemented in many areas in the next years.

The system used is based on a 800 DC bus voltage reference and a power converter of 10 kVA, which is not much and wouldn't represent the amount of energy provided with a photovoltaic plant, but would be useful to get an idea of how the sunlight can be used to provide energy to an AC grid.

It is also remarkable how with simplified models it is possible to simulate what in reality is much complex. Both the converter and the photovoltaic models have been implemented by using reduced models, avoiding the IGBTs, for example. With those the behavior of the real systems can be represented, making the work much easier.

The software also benefits from the simplicity of the model. It has been appreciated how each time the model was getting more elaborated, more time was needed by Simulink to execute it and to make the whole simulation, and more errors were probable to appear, so is it necessary to be accurate with the implemented blocks.

In order to optimize the process and acquire the maximum power as possible, methods provided by engineering as the MPPT are very useful to be incorporated. The more efficient the renewable system is, the more probable of being implemented around the world would be. After all, the main objective would be to leave behind the non-renewable sources to implement these kinds of energies. So, an economically feasible project that provides the optimum power is needed to achieve it. Obviously, not everywhere the presence of sunlight is abundant, but other energies as wind or hydraulic power could be used instead.

## 9. Acknowledgements

Most mainly, I must express my thanks to my work tutor, Marc Cheah, who has been helping me through the whole process by kindly showing me his support and attention. My electronic skills were not very advanced, and I had hardly used the simulation software, so my tutor's guidance was essential to be able to develop the project. Therefore, I would also like to acknowledge the CITCEA department, concretely to Oriol Gomis, who gave me advice in the first place.

I would also like to thank my university colleagues, who brought up my interests in the field of photovoltaic panels. Renewable sources had always been of great concern to me, but with their work the questions of how those systems worked came up to me.

## 10. References

- [1] MADURAI R., *The Motivation for Renewable Energy and its Comparison with Other Energy Sources: A Review*. Available: [https://www.researchgate.net/publication/329979101\\_The\\_Motivation\\_for\\_Renewable\\_Energy\\_and\\_its\\_Comparison\\_with\\_Other\\_Energy\\_Sources\\_A\\_Review](https://www.researchgate.net/publication/329979101_The_Motivation_for_Renewable_Energy_and_its_Comparison_with_Other_Energy_Sources_A_Review). [Accessed 6 June 2020]
- [2] EGEEA-ALVAREZ A., JUNYENT-FERRÉ A. and GOMIS-BELLMUNT O., *Active and reactive power control of grid connected distributed generation systems*.
- [3] GRADELLA-VILLALVA M., RAFAEL-GAZOLI J. and RUPPERT-FILHO E., *Comprehensive Approach to Modeling and Simulation of Photovoltaic Arrays*.
- [4] HUAN-LIANG T., CI-SIANG T. and YI-JIE S., *Development of Generalized Photovoltaic Model Using MATLAB/SIMULINK*.
- [5] SAID S., MASSOUD A., BENAMMAR M. and AHMED S., *A Matlab/Simulink-Based Photovoltaic Array Model Employing SimPowerSystems Toolbox*
- [6] *MPPT Algorithm*. <https://es.mathworks.com/solutions/power-electronics-control/mppt-algorithm.html>

